Exhumation of high-pressure rocks: role of late faulting (Eastern Ossa-Morena Complex, Iberian Massif)

Rubén Díez Fernández[1], Irene Novo-Fernández[2], Diana Moreno-Martín[2], Ricardo Arenas[2], Esther Rojo-Pérez[2], Luis Miguel Martín Parra[1], Jerónimo Matas[1]

[1]Departamento de Geología y Subsuelo, CN-IGME-CSIC, Spain.

[2]Departamento de Mineralogía y Petrología and Instituto de Geociencias (UCM-CSIC), Universidad Complutense, Madrid, Spain.

Corresponding author: r.diez@igme.es

ABSTRACT

Exhumation of high-pressure (P) rocks may require a long path and multiple deformation phases. During this journey, late faults and folds can introduce changes to the primary tectonic stacking and lead to misleading conclusions regarding subduction polarity and plate reconstructions. This hypothesis has been tested positively via mapping and structural analysis in the eastern section of the Central Unit (Eastern Ossa-Morena Complex, Iberian Massif), which comprises Devonian high-P rocks subducted during the Variscan Orogeny. Following subduction beneath Gondwana, exhumation was assisted by in-sequence underthrusting of the continental crust, along with thinning of the overlying and formerly accreted crust. Convergence persisted and was accommodated by Gondwana-directed, out-of-sequence thrusts. Subsequent extension favored erosion and basin inception during the Early Carboniferous, whereas further convergence produced late folding and faulting during Late Carboniferous sinistral transpression. Late faults

duplicated the Devonian suture zone several times, producing a series of closely-spaced exposures of a single suture. The manner in which late faults affected the Devonian suture produced an outcome that could be mistaken for a collection of individual suture zones. Late faults may distort the primary relationships between upper and lower plates; however, they provide a geometry-based approach for restoring the primary geometry of suture zones.

Keywords: Suture zone; Continental subduction; Exhumation; Thrusts; Variscan Orogen; Iberian Massif

1. INTRODUCTION

Much effort has been devoted to understanding the exposure of high-pressure (P)/low- to mid-temperature (T) rocks (blueschists and eclogites) on the surface to identify the processes responsible for their exhumation through a subduction channel and up to the lower-middle crust (Agard et al., 2009; Díez Fernández et al., 2011; Gerya et al., 2008; Gerya et al., 2002; Jolivet et al., 2003; Warren, 2013). Such exhumation is conceived as a transient event after perturbations in the subduction zone (Guillot et al., 2009). A complementary line of thinking acknowledges the exhumation of some subducted rocks through diapiric ascent away from subduction channels (Little et al., 2011; Malusà et al., 2015; Maierová et al., 2021). In any case, deep-seated rocks follow paths within or away from the subduction channel, and the dynamics of the latter seem to control much of the path that high-P rocks follow back to the surface (Ernst and Liou, 2008; Willner et al., 2002; Yamato et al., 2007). Understanding high-P rock exhumation requires the entire set of processes that have operated from the mantle to the uppermost crust to be revealed (e.g., Platt, 1993). Late steps through the exhumation path occur in the middle and, more importantly, in the upper crust. Exhumation in the upper crust is mostly caused by a combination of erosion and normal faulting. However, erosion may act not only on crust sections attenuated by normal faults (e.g., Strak et al., 2011), but also on sections affected by thrusts and folds (e.g., Avouac, 2003), giving ways for exhumation to occur during crustal thickening.

The onset of continental subduction heralds continental collisions. In this particular case, early high-P rock exhumation is controlled by subduction channel dynamics, but late exhumation can be unrelated and controlled by processes that may eventually operate across the hinterland of collisional orogens, and are not only localized across the root of any of their suture zones. This would encompass later faulting (either thrusts, normal, or strike-slip faults), typical for advanced stages in an ongoing collisional orogen (Vanderhaeghe, 2012). In this context, shortening is usually accommodated by thrusting upon later convergence long past the onset of the collisional stage. Normal faults can drive the exhumation of lower and middle crust rocks during thermal and gravitational re-equilibration after (or during) crustal thickening (e.g., orogenic collapse) (Dewey, 1988; Díez Fernández et al., 2012; Rey et al., 2001), whereas strike-slip faults may be formed at any stage during orogenesis to accommodate lateral displacements (Pavlis et al., 2004; Shelley and Bossière, 2000; Woodcock and Daly, 1986).

Late faults and folds have the potential to distort previous structures. Faults operating on high-P rocks exhumed to middle and upper crust depths can modify structures generated during previous decompression (e.g., within or away from the subduction channel), thus complicating the reconstruction of subduction zone dynamics (Díez Fernández et al., 2021a; Díez Fernández et al., 2022b). Folds modify (curve) the primary geometry of preexisting planar features. This makes interpretation of the pre-fold record challenging. Here, we present a case example from the Variscan Orogen (SW

Iberian Massif) to illustrate the intense re-deformation distortion of early collisional structures affecting high-P rocks formed in a continental subduction zone once they have returned to middle-upper crust depths. We discuss the processes and structures responsible for the latest exhumation and how such distortions may have contributed to misleading interpretations of subduction zone dynamics in the Variscan Orogen.

2. GEOLOGICAL SETTING

The Iberian Massif represents a piece of the Western European Variscan Orogen, which was formed after the collision of Laurussia, Gondwana and their peripheral terranes during the late Paleozoic (Figs. 1a and 1b; Díez Fernández et al., 2016; Kroner and Romer, 2013; Matte, 2001; Schulmann et al., 2014). This collision resulted in the amalgamation of continental terranes separated by two types of suture zones, those along which Gondwana-derived terranes are juxtaposed and those where Gondwana-derived terranes are juxtaposed against pieces of continental crust with Laurussian affinity. The SW Iberian Massif contains both types of suture zones, some of which include high-P rocks that attest to the burial of continental crust to mantle depths (Abalos et al., 1991b; Arenas et al., 2021; López Sánchez-Vizcaíno et al., 2003; Novo-Fernández et al., 2021; Pereira et al., 2010a). This is the case for the Central Unit, which strikes NW-SE and is surrounded by mid- to low-P rock assemblages and Variscan syn-orogenic strata (Fig. 1c) (Abalos, 1990; Azor, 1994).

The lower and upper plates of the suture zone exposure, represented by the Central Unit, are a matter of debate. It is accepted that the lower plate (Iberian Autochthon in Figure 1b) comprises at least two rock assemblages in SW Iberia: the Albariza-Bembézar Succession and the Azuaga Formation (Azor et al., 1994; Díez Fernández and Arenas, 2015). This pair shows affinity with some rock units of the Central Iberian Zone

(Fuenlabrada et al., 2021; Solís-Alulima et al., 2022) and is also referred to as Iberian Autochthon. The Iberian Autochthon is thought to have been structurally and paleogeographically connected to the same section of the margin of Gondwana (i.e., the Central Iberian Zone), which represents the lower plate of the Variscan suture zone exposed in the NW Iberian Massif (Díez Fernández and Arenas, 2015; Díez Fernández and Arenas, 2016). This connection formed during the suturing and building of a Devonian accretionary system, which included, in ascending order, the following Variscan nappe stacks: (i) a lower plate with Gondwanan affinity (referred to as the Autochthon), (ii) far-traveled pieces of subducted continental crust (Lower Allochthon, including the Central Unit), (iii) ophiolites (Ophiolitic or Middle Allochthon), and (iv) an upper plate with Gondwanan affinity (Upper Allochthon) (Arenas et al., 2016; Díez Fernández et al., 2016).

The Central Unit and surrounding rocks have Gondwanan affinity; therefore, it is an example of an intra-Gondwanan suture zone, that is, a suture that is interpreted to have formed after the closure of a peripheral (marginal) basin located along the margin of Gondwana (Díez Fernández and Arenas, 2015; Simancas et al., 2009). Most of the Central Unit is bounded by late Variscan faults, namely, the Azuaga Fault to the SW and the Matachel Fault to the NE (Fig. 1; Abalos and Eguiluz, 1991; Azor et al., 1994; Díez Fernández et al., 2021a; Díez Fernández et al., 2022b). These faults belong to the so-called Coimbra-Badajoz-Córdoba shear zone (Burg et al., 1981), which is a sinistral transpressional system that formed at a late stage during the Variscan orogeny (Abalos and Eguiluz, 1991; Azor et al., 1994; Díez Fernández et al., 2021a; Pereira et al., 2010b). These faults cut across the folded internal structure of the Central Unit, which is defined by Early Carboniferous mylonitic foliation formed during exhumation after Devonian high-P (eclogite facies) metamorphism (Abati et al., 2018; Azor et al., 1994; Díez

Fernández and Arenas, 2015; Pereira et al., 2010a). The assemblage of rocks that constitute the Central Unit includes meta-sedimentary and meta-igneous rocks, with protolith ages ranging between the Ediacaran and Ordovician (Abalos, 1990; Abati et al., 2018; Azor, 1994; Ordóñez Casado, 1998). High-P metamorphism ranges between blueschist facies (e.g., Arenas et al., 2021) and eclogite facies conditions (e.g., Abalos et al., 1991b; López Sánchez-Vizcaíno et al., 2003; Pereira et al., 2010a). Post-high-P metamorphism ranges between greenschist, amphibolite, and granulite facies conditions, including partial melting in some sections (e.g., Abalos et al., 1991b; López Sánchez-Vizcaíno et al., 2003; Pereira et al., 2010a; Arenas et al., 2021; Díez Fernández et al., 2021a).

The Upper Allochthon (upper plate; Upper Allochthonous Units in Figure 1b) bears an imprint of tectonomagmatic processes related to the Cadomian orogeny (from Ediacaran to Cambrian; Arenas et al., 2018; Díez Fernández et al., 2022a; Díez Fernández et al., 2019; Eguíluz et al., 2000; Quesada, 1990; Rojo-Pérez et al., 2022). Variscan tectonics is recorded in all of its pre-Variscan rock assemblages, which range from the Ediacaran to the Devonian (e.g., Díez Fernández et al., 2021b; Eguíluz et al., 2000; Expósito et al., 2002; Expósito et al., 2003; Martínez Poyatos et al., 2001). The protoliths of the Autochthon show a similar age range (Ediacaran to Devonian), the older protoliths being affected by pre-Variscan (Ordovician) tectonomagmatic processes (e.g., Azor et al., 2012; Solís-Alulima et al., 2020). The Central Unit is surrounded by syn-orogenic strata, which span from the Tournaisian to the Gzhelian (Azor, 1994; Martínez Poyatos, 2002; Matas et al., 2015). Most series are affected by Variscan deformation and metamorphism, and some even contain Variscan igneous rocks (Armendariz et al., 2008; Díez Fernández et al., 2021a). Carboniferous syn-orogenic strata can be found covering the Variscan upper and lower plates. The older units were deposited in marine environments (e.g., Armendariz et al., 2008), whereas the younger units were formed in intramountainous settings (Wagner, 2004).

3. MATERIALS AND METHODS

Geological mapping was carried out on a 1:10,000 and 1:25,000 scale using a rugged tablet assisted by GPS and GIS technologies. Base maps (topographic and orthophotos) were downloaded from the Spanish National Geographical Survey (http://centrodedescargas.cnig.es). Figure 2 shows a new geological map and serial cross sections across the most representative structures, whereas Figure 3 is an adapted version of the geological map published by Díez Fernández et al. (2021b) from an adjacent area located to the north (see the location of both maps in Figure 1).

The bedrock of the study area was divided into pre-orogenic and syn-orogenic rocks with respect to the Variscan Orogeny. Pre-orogenic rocks are grouped into tectonostratigraphic units that consist of rock members with equivalent Variscan tectonometamorphic evolutions. Each tectonostratigraphic unit is considered to be separated from the other units by a major crustal-scale fault. This subdivision is based on the interpretation that each tectonostratigraphic unit represents a major tectonic slice within an imbricate system that hosts a suture zone formed during the early stages of the Variscan subduction/collision (see data and discussion below). The location and nature of major faults are based on structural analysis and metamorphic evolution.

The structural data used in large-scale (km-scale) structural analyses and geometrical interpretations comprise field observations and the selection of domains where structures are well preserved. The selected domains are referred to as Reference Points (RP) in the text. Unless otherwise indicated, the main foliation within each lithological assemblage was the reference to determine and describe a lower or upper structural position across the same assemblage. The shear sense criteria in field outcrops were established based on sections as normal as possible to the local vorticity vector (roughly parallel to the stretching lineation in this study). Presentation of structural data on stereographic projections (lower hemisphere and equal area) was performed using Stereonet v. 11.3.1 (R.W. Allmendinger, https://www.rickallmendinger.net/stereonet; Cardozo and Allmendinger, 2013).

4. TECTONOMETAMORPHIC RECORD AND TIME FRAME

4.1. Autochthon

The nature of the main foliation in the Albariza-Bembézar Succession varies from gneissic layering in the ortho- and paragneisses that occupy the lower structural positions to schistosity at the intermediate and upper structural levels (Fig. 4a). In meta-sedimentary rocks, metamorphic garnet, staurolite, and sillimanite form part of the main foliation. Minor melanosomes and andalusite are also present. In the Azuaga Formation, the main foliation is slaty to phyllitic cleavage that grades into a poorly developed schistosity (vague tectonic banding) down structure (Fig. 4b). The main foliation may include quartz, plagioclase, chlorite, muscovite, biotite and minor garnet. The main foliation includes mineral and stretching lineations. In meta-sedimentary rocks, the stretching lineation is marked by quartz ribbons, elongated aggregates of metamorphic minerals (sillimanite, garnet, biotite, and muscovite), or by boudinaged layers of meta-sandstone or veins. The elongated shape of syn-kinematic minerals (sillimanite, garnet, and biotite) defines the mineral lineation. The mineral and stretching lineations are consistently parallel and show a trend between N-S and NW-SE (Fig. 5a). The main foliation includes asymmetric structures, such as C-S fabrics, C’-planes, C’-S fabrics, sigma-type objects (porphyroclasts), asymmetric pressure shadows around porphyroblasts, and oblique fabrics at the microscale. Dominant shear sense is top-to-the-SE and S.

The main foliation in the Autochthon is axial-planar to the folds. The obliquity between bedding and the main foliation suggests that the major folds are overturned with an intersection lineation that trends NW-SE (Fig. 5b), parallel to the hinge lines of the parasitic folds associated with the main foliation (figs. 4c and 5c). Refolding (see section 4.5) and a lack of good way-up criteria and marker layers prevented the establishment of major fold vergence and asymmetry. However, if the Azuaga Formation is younger than the Albariza-Bembézar Succession, the upper structural position of the former suggests a major normal fold limb in the study area.

The strain is heterogeneous and generally increases in the down structure. Protoliths of the Azuaga Formation exhibit bedding (Fig. 4b), whereas the Albariza-Bembézar Succession is pervasively deformed (strain distribution is not markedly heterogeneous), and bedding is largely obliterated (Fig. 4a). The Azuaga Formation recrystallized under greenschist facies conditions characterized by garnet and minor biotite. The lower part of the Albariza-Bembézar Succession reached partial melting conditions, whereas the upper part recrystallized under amphibolite facies conditions (within the garnet-staurolite zone; González del Tánago and Arenas, 1991), followed by high-T and low-P recrystallization (andalusite stability field; Azor and Ballèvre, 1997). Overall, the metamorphic grade defines a telescoped normal zonation.

4.2. Lower Allochthon

The Lower Allochthon (Central Unit) exhibits a main, penetrative, mylonitic foliation that wraps around pods of (retro)eclogite and rocks that preserve mineral assemblages formed under high-P and low-T conditions (Abalos et al., 1991b; Arenas et al., 2021). Tectonic fabrics older than the main foliation were preserved as preferentially oriented and retrogressed mineral assemblages within (retro)eclogite pods and as mineral inclusions within albite and garnet porphyroblasts. The main foliation was formed under amphibolite to greenschist facies conditions during decompression and is defined by different mineral assemblages depending on the lithology (see Abalos (1990) and Azor (1994) for further petrographic details). The main foliation in migmatites, which are exclusive to the Serie Negra Group, is defined by alternating bands of (granitic) leucosome and (biotite-rich) melanosome that bind variably thick bodies of paleosome made of sillimanite-bearing paragneiss, whose main foliation is also parallel to the migmatitic banding (Fig. 4d). Granitic veins and pods are abundant near and in migmatite exposures. The deformation of these granitoids varies between being nearly unaffected by the main foliation and being flattened, stretched and boudinaged during foliation development.

Minerals oriented parallel to the main foliation also define mineral and stretching lineations (Fig. 4e). In meta-sedimentary rocks, this stretching lineation is marked by quartz ribbons, elongated aggregates of metamorphic minerals (sillimanite, garnet, biotite, and muscovite), or by boudinaged and/or lens-shaped layers of quartzite, meta-sandstone, meta-basites, or veins. The elongated shape of syn-kinematic minerals such as sillimanite, garnet, biotite, and albite define the mineral lineation. In meta-igneous rocks, the orientation of the stretching lineation is represented by the long axis of pre-tectonic objects such as porphyroclasts, xenoliths, or boudinaged dikes or veins. Both mineral and stretching lineations in meta-sedimentary and meta-igneous rocks are consistently parallel and trend between NW-SE, N-S, and NNE-SSW (figs. 5d and 5e). The intensity of the linear fabric of these rocks varies such that LS (most common), S and L-tectonites are present.

Protoliths of the Lower Allochthon are commonly pervasively deformed, especially meta-sedimentary ones (Fig. 4f), into high-strain tectonites. Low-strain rocks are locally preserved in the orthogneisses, although the heterogeneous strain is generally high (e.g., Abalos and Eguiluz, 1989; Abalos and Eguiluz, 1990). The main foliation is axial planar to near-isoclinal folds (Fig. 4g), which are defined by the compositional banding of the rocks, either primary (bedding in meta-sedimentary rocks) or tectonic (banding in gneisses). The development of the main foliation includes asymmetric structures, such as C-S fabrics, C'-planes, C'-S fabrics, sigma-type and delta-type objects (porphyroclasts), asymmetric pressure shadows around porphyroblasts and porphyroclasts, asymmetric folds, oblique fabrics at the microscale, and fractured grains (porphyroclasts). The dominant shear sense is top-to-the-SE and -S (Fig. 4h).

Early metamorphism within the Lower Allochthon reached eclogite facies conditions in some sections (Abalos et al., 1991b; Pereira et al., 2010a) and blueschist facies conditions in others (Arenas et al., 2021). The main foliation also developed under different conditions, ranging between partial melting (migmatitic paragneisses; Fig. 4d) and greenschist to amphibolite facies conditions (Abalos et al., 1991b; Arenas et al., 2021; Pereira et al., 2010a). The abundance of migmatites and magmatism synchronous with the main foliation decreases rapidly towards the upper structural levels of the Ediacaran sequences, in less than 500 m across the structure. The gneissic banding that dominates the lower sections (Serie Negra Group) progressively turns into a finer-grained schistosity upsection. Overall, the metamorphism associated with the main foliation in the Serie Negra Group of the Lower Allochthon decreases upsection and defines a likely telescoped normal zonation.

4.3. Upper Allochthon

The main foliation is a slaty cleavage that grades into spaced and rough cleavages marked by reoriented sedimentary clasts of quartz, feldspar, plagioclase, and mica, and the preferred orientation of newly formed chlorite and sericite. The main foliation is oblique to bedding.

The strain related to the main foliation is very low compared with that of the rest of the units. It is still possible to observe well-preserved fossils in sections away from the major faults.

4.4. Syn-orogenic meta-sedimentary rocks

Only the older units of the Early Carboniferous sedimentary rocks (C1, Culm facies) exhibit penetrative (axial plane) foliation. This foliation is defined by newly-formed quartz, sericite, muscovite, and chlorite and by mineral grains (clasts) of the protolith reoriented parallel to the fabric. In the meta-conglomerates, the foliation is an anastomosing spaced cleavage, whereas in meta-sandstones and meta-pelites, it appears as a regularly spaced cleavage.

4.5. Late crenulation cleavage

The main foliation in the pre-orogenic rocks is transposed by a near-vertical crenulation cleavage that strikes NW-SE (Fig. 6a). This fabric is best developed in meta-sedimentary lithologies and is axial-planar to upright folds on all scales (fig. 4a, 4b, and 4d). Fold axes trend NW-SE and plunge shallowly either to the NW or SE (figs. 6b, 6c, 6d, and 6e). The crenulation cleavage is accompanied by a crenulation lineation that trends NW-SE (Fig. 6a), subparallel to the strike of the crenulation cleavage and to mesoscale upright fold axes (Fig. 6).

This sub-vertical crenulation cleavage is defined by reoriented minerals from previous foliation and neo-blasts of quartz, sericite, muscovite, and chlorite. This cleavage and associated folds are parallel and geometrically similar to the axial planar foliation and folds in the syn-orogenic Culm facies rocks. Accordingly, they are considered equivalent. The metamorphic conditions accompanying the development of this fabric were estimated at greenschist facies (2-5 kbar; Abalos et al., 1991a).

4.6. Deformation ages

The main foliation in the Autochthon must be post-Cambrian (age of the younger rocks with this fabric). $^{40}Ar/^{39}Ar$ dating of the main foliation in the Albariza-Bembézar Succesion (amphibole in meta-basites and muscovite in schists) yielded plateau ages of c. 392 Ma, 385 Ma, 359-351 Ma and 336 Ma (Azor et al., 2012; Dallmeyer and Quesada, 1992), so Variscan deformation and cooling in the Autochthon ranges from the Late Devonian to at least the Early Carboniferous. U-Pb zircon dating of migmatites of the Albariza-Bembézar Succession yielded crystallization ages between c. 497 Ma (Azor et al., 2012) and c. 478 Ma (Solís-Alulima et al., 2020), which, together with the intrusion of Ordovician granitoids (Azor et al., 2016; Solís-Alulima et al., 2020) and some $^{40}Ar/^{39}Ar$ ages obtained from amphiboles (c. 482 Ma; Azor et al., 2012) are considered to represent a pre-Variscan tectonothermal imprint in the Autochthon (e.g., Dallmeyer and Quesada, 1992). In our case study, the first deformation recorded in the Azuaga Formation is also the first one that affected Devonian strata (Díez Fernández et al., 2021b); therefore, the pre-Variscan tectonothermal imprint appears to be missing or negligible in this part of the Autochthon.

The age of high-P metamorphism in the Lower Allochthon has been estimated to be 377 ± 19 Ma (U-Pb metamorphic zircon in retro-eclogites; Abati et al., 2018). This Variscan age matches the age range obtained in a previous study (c. 380-350 Ma, U-Pb zircon dating; Ordóñez Casado, 1998) and is roughly in agreement with previous work that obtained ages of either slightly older (427 ± 45 Ma, U-Pb zircon dating in retro-eclogite; Schäfer et al., 1991) or slightly younger (c. 370-360 Ma, $^{40}Ar/^{39}Ar$ dating; Quesada and Dallmeyer, 1994). The radiometric ages for the development of the main foliation of the Lower Allochthon are ca. 355 Ma (Rb/Sr dating of mylonites formed during post-high-P retrogression; García Casquero et al., 1988), and c. 340-333 Ma ($^{40}Ar/^{39}Ar$ mica and U-Pb zircon dating of post-high-P migmatization; Abati et al., 2018; Pereira et al., 2010a; Pereira et al., 2012).

In SW Iberia, Variscan granitoids dated at c. 318 Ma (Pereira et al., 2010b) display a fabric correlated with near-vertical crenulation cleavage elsewhere, which is cut by younger Variscan plutons dated at c. 306 Ma (Solá et al., 2009). In our study area, late crenulation cleavage is associated with upright, NW-SE trending folds, which affect the youngest syn-orogenic series dated at Moscovian (c. 315-307 Ma). Accordingly, deformation related to late crenulation cleavage occurred (at least) between c. 318 and 307 Ma.

5. RECOGNITION OF MAJOR FAULTS

Some of the major structures developed in the study area are not directly exposed (due to intense weathering). However, their existence, geometry, and relative timing were established based on a detailed structural mapping (Fig. 2).

5.1. Early thrusts

Early thrusts are identified by Variscan high-P rocks (Lower Allochthon) structurally overlying Variscan mid-P rocks (Autochthon), in the absence of Carboniferous syn-orogenic strata, and in the presence of serpentinites (meta-peridotites) (RP-1, Figure 2). Serpentinites also occur within the Ediacaran sections of the Lower Allochthon (RP-2, Figure 2), and they separate higher-grade sequences (sillimanite and partial melting) from structurally underlying lower-grade sections. In the absence of meta-peridotites, these thrusts were tentatively mapped by identifying the sections affected by more intense strain. Additionally, the migmatites and the rest of the rocks that form part of the Ediacaran section of the Lower Allochthon (Serie Negra) lie on top of the younger (Paleozoic) and colder sections of the Lower Allochthon, such as the (garnet-bearing) mica-schists (RP-3, Figure 2). The thrust required to explain such metamorphic juxtaposition has also been considered as early Variscan.

5.2. Early extensional low-angle faults

The main foliation in the Lower Allochthon and Autochthon is axial-planar to isoclinal folds on the meso- (figures 4c and 4g) to macroscale (e.g., RP-4, Figure 2). However, the axial trace (RP-4, Figure 2) and both fold limbs (RPs-5 and 6, Figure 2) converge and are cut-off by a fault that reminds us of an early thrust (RP-1, Figure 2). The trace of the latter fault, referred to as the Villanueva detachment, no longer represents the trace of an early thrust (needed to explain the current Allochthon-Autochthon juxtaposition), but the trace of a later, low-angle fault that excised a former tectonic stack previously built by early thrusts (see section above).

The main foliation in the Lower Allochthon and Autochthon is sub-parallel to the trace of the Villanueva detachment and formed under roughly similar metamorphic conditions (greenschist to amphibolite facies). The Villanueva detachment cuts structurally lower sections of the Lower Allochthon in the SE (RP-5, Figure 2) than in the NW (RP-4, Figure 2), and produces wedging of the Lower Allochthon orthogneisses to the NW (RP-6, Figure 2). To the S, the same (Ediacaran) section of the Lower Allochthon does not rest onto the Autochthon, but onto younger, yet underlying sections of the Lower Allochthon (RP-3, Figure 2). This implies N-NW wedging of the Lower Allochthon as a whole (section C-C' in Figure 2). Accordingly, the fault that defined its base before late upright folding (Villanueva detachment) dipped either steeper to the S-SE or shallower to the N-NW than the (missing) early thrust that transported the Lower Allochthon onto the Autochthon. If an N-NW-dipping paleo-geometry of the Villanueva detachment is combined with the top-to-the-SE and -S shearing associated with the main foliation in the Lower Allochthon and Autochthon, the structural discontinuity between Autochthon and Lower Allochthon has thrust fault kinematics. However, no tectonic duplication was observed in relation to the Villanueva detachment. In contrast, if the kinematics of the main foliation is combined with an original S-SE-dipping Villanueva detachment, the fault has normal fault kinematics and the wedging (excision) of the Lower Allochthon can be linked to extension.

5.3. Early out-of-sequence thrusts

Early out-of-sequence thrusts cut across the trace of the early thrusts (RPs-7, 8 and 9, Figure 2), duplicate the foliated Lower Allochthon (RPs-10 and 11, Figure 2) and Autochthon (RP-12, Figure 2), and emplace the Autochthon again onto the Lower Allochthon. These features separate these thrusts from the early thrusts, but both originally had a relatively shallow-dipping orientation, which is either directly observed in the field or can be inferred from their upright folded nature where affected by subsequent deformation (RPs-7, 8, and 12, Figure 2). The original overall low-angle geometry of these thrusts is further supported by a klippe of Autochthon south of Villanueva del Rey (RP-12, Figure 2).

The early out-of-sequence thrusts cut across the previous structures in the Autochthon and Allochthon and include flats (faults that tend to be parallel to the previous structure; RP-8; Figure 2) and ramps (faults that are markedly oblique to the previous structure RP-9, Figure 2). The lower structural section of the hanging wall of the early out-of-sequence thrusts consists exclusively of Autochthon rocks. In some sections, these thrusts cut upward through the internal structure of the Autochthon (RP-13, Figure 2), whereas in other parts, they seem to be the opposite (RP-9, Figure 2). Similarly, the Lower Allochthon occupies the footwall of these thrusts, which progressively intercept lower structural sections of the Lower Allochthon towards the NE (RPs-7, 8 and 9, Figure 2), as they cut through earlier steeper SW-dipping thrusts.

5.4. Late out-of-sequence reverse faults and strike-slip shear zones

The late reverse faults differ from the other earlier-formed reverse-slip faults in the study area in that they are parallel and cut upright folds as defined by primary contacts (sedimentary or igneous) and main foliation (Fig. 2). These faults generally strike NW-SE and dip steeply SW. These faults form along the shared steep limbs between upright (hanging wall) antiforms and upright (footwall) synforms (RPs-1 and 12, Figure 2) and collectively define an imbricate fault set with tectonic transport directed to the NE (RP-14, Figure 2).

The strike, kinematics, and relationships between strike-slip faults and late out-of-sequence reverse faults are complicated. The most common set of strike-slip faults strikes NE-SW and is sinistral (as inferred from horizontal separations). The main sinistral-slip fault defines the northern boundary of the Villaviciosa – La Coronada

Complex (RP-15, Figure 2). This fault could represent the eastern continuation of the Matachel Fault (Azor et al., 1994). The strike of this fault is dominantly NW-SE, but it runs E-W and SW-NE towards the eastern part of the study area (RP-16, Figure 2). Slickensides related to this fault (three *in situ* observations) are near-vertical, parallel to its trace, and accompanied by very shallowly NW-plunging slickenlines (~5°) (two *in situ* observations). This sinistral strike-slip fault seems to define a tear fault system with respect to the late out-of-sequence reverse faults (RP-6, Figure 2) for which we cannot rule out a component of strike slip. A set of dextral, subsidiary, strike-slip faults strike NW-SE (RP-17, Figure 2).

The strike of the late out-of-sequence reverse faults is clockwise from the major fault with which they converge (e.g., RP-15, Figure 2). The main foliations and axial traces of the upright folds depict a similar *en echelon* pattern (e.g., RP-10, Figure 2). The same obliquity and pattern can be observed between these faults and the upright folds located at their hanging walls and footwalls (e.g., RP-18, Figure 2).

6. DISCUSSION

6.1. From deep-seated to surface: structural evolution of high-P rocks

The structures and mapped tectonostratigraphy described in previous sections can be integrated into a tectonic model comprising five major tectonic events.

6.1.1. Subduction/accretion of Gondwanan crust

The main evidence for the early subduction of the Gondwanan crust (Figure 7a) in the study area is the mid- to Late Devonian high-P metamorphism (eclogite to blueschist facies conditions) recorded in the Lower Allochthon (Abati et al., 2018; Ordóñez Casado, 1998; Quesada and Dallmeyer, 1994). Deep continental subduction of the Ediacaran units of the Lower Allochthon was followed by its (early) thrusting over the younger and colder (less-buried?) units of the Lower Allochthon, namely mica schists and garnet-bearing mica schists (RP-3, Figure 2). The garnet-bearing mica schists bear imprints of Variscan high-P metamorphism (Abalos et al., 1991b; Arenas et al., 2021; Azor, 1994); therefore, the onset of early thrusting occurred under a high-P gradient. In addition to the initial burial beneath the mantle, early thrusting represents the decoupling of lower plate pieces in the subduction channel.

The lack of high-P metamorphism in the Autochthon rocks and its early overthrusting by the Lower Allochthon (RPs-1 and -18, Figure 2) indicate that subsequent tectonic juxtapositions occurred under different metamorphic conditions, so the decompression and exhumation of the high-P rocks of the Lower Allochthon was in an advanced stage. The main foliation in the Lower Allochthon and Autochthon could be entirely related to this phase of tectonometamorphic evolution. However, some key observations suggest otherwise. These fabrics have yielded radiometric ages ~25-40 m.y. younger than the age of high-P metamorphism in the Lower Allochthon (García Casquero et al., 1988; Pereira et al., 2010a). The main foliation in the Lower Allochthon and Autochthon is parallel to the presumed early thrust contact between them (RPs-4, -5, and -6, Figure 2), which attenuates the tectonic stack (see description of the Villanueva detachment in Section 5.2). Accordingly, we believe that the main foliation in the Lower Allochthon and Autochthon was formed in relation to a post-early thrusting event.

The serpentinite lenses (meta-peridotites) within the Lower Allochthon (RPs-8 and -9, Figure 2) and along its interface with the Autochthon (RP-1, Figure 2) probably represent slices of mantle incorporated at this stage. Alternatively, the serpentinites were inherited from Ediacaran accretionary processes, as recently described for the Serie Negra Group in SW Iberia (Arenas et al., 2018; Díez Fernández et al., 2022a; Díez Fernández et al., 2019). The upper plate of the Variscan subduction system is inferred to be represented by the Upper Allochthon (Díez Fernández and Arenas, 2015; Díez Fernández et al., 2021b), which experienced little Variscan tectonic loading compared with the Lower Allochthon and Autochthon.

6.1.2. Early attenuation of the orogenic crust

The Villanueva detachment (RP-1, Figure 2) and the main foliation of the Lower Allochthon and Autochthon account for crustal attenuation after early thrusting. The primary dip-direction of the Villanueva extensional detachment suggests that its related tectonic transport had a southerly component. The trend of stretching lineations in the main foliation of the Lower Allochthon and Autochthon is dispersed between NE-SW, N-S, and NW-SE trends (Fig. 5f), with a dominant component of shearing directed to the S. This dispersion is compatible with the regional trend of late upright folds and strike-slip faults, which are NW-SE. Collectively, these lineations seem to define a set of lines that originally trended N-S, and most likely NE-SW (Fig. 5f), and were reoriented to a linear fabric attractor (Passchier, 1997) trending NW-SE (see an equivalent example in the Lower Allochthon published by Díez Fernández and Martínez Catalán, 2012). Accordingly, the tectonic flow that can be inferred for this extensional event was directed to the S and SW.

It is possible that they represent a phase of extensional collapse responsible for a severe lithospheric attenuation. Although this extension may be related to the development of thermal domes in other parts of SW Iberia (e.g., Pereira et al., 2009; Dias da Silva et al., 2018), it reflects the subhorizontal ductile flow of an increasingly constricted orogenic wedge upon progressive underthrusting of additional crust to its base

(Figure 7b; Díez Fernández et al., 2016). This interpretation does not exclude the possibility that thermal domes formed coevally and/or eventually afterwards.

6.1.3. Early out-of-sequence thrusting

This event introduced a major change in the makeup of the Variscan orogenic wedge (Figure 7c). The early thrust that transported the Lower Allochthon onto the Autochthon was duplicated by at least one later, primarily shallowly-dipping, out-of-sequence thrust (RPs-9, -13, and -11, Figure 2). The shallowly dipping geometry can be inferred from the fact that this out-of-sequence thrust and other imbricates are folded into upright synforms (RPs-7 and -12, Figure 2) together with bedding and foliations in the study area. Moreover, the trace of this fault defines ramps and flats that cut the lower structural levels of its footwall (Lower Allochthon) and hanging wall (Autochthon) to the NE (RPs-13, -8, and -9, Figure 2). Thus, we propose an overall SW-dipping, staircase thrust geometry that is slightly more inclined to the SW than the former tectonic wedge it cuts across and duplicates (Fig. 7). If so, the overall geometry of the previous tectonic wedge was also SW-dipping, consistent with an assemblage pervasively affected by S- to SW-directed extensional flow (note the reoriented nature of stretching lineations pointed out in section 6.1.2).

The hanging wall of this early out-of-sequence thrust set covered the entire area represented in Figure 2, from the sections located to the S of the main strike-slip shear zone (RP-11, Figure 2), passing through the klippe in the central part (RP-12, Figure 2), to at least the section covered with Carboniferous syn-orogenic sedimentary rocks. The current juxtaposition of the Lower Allochthon against the Autochthon, covered by syn-orogenic rocks, via late out-of-sequence reverse faults (see below) implies that the pre-Variscan rocks of that part of the study area represent hanging wall remnants of the early out-of-sequence thrust. The Autochthon exposed in that area (e.g., RP-19, Figure 2) would be the continuation of the Autochthon that occupies the hanging wall to the early out-of-sequence thrust exposed to the SW (e.g., RP-9, Figure 2). The Culm facies syn-orogenic strata (C1 in Figure 2) rest unconformably exclusively on top of the hanging wall of this early thrust system. These syn-orogenic strata occur in both the SW and NE of the study area. Therefore, the hanging wall of the early out-of-sequence thrust system occupied the topmost structural position and covered the entire study area (Figure 7c) before the Culm series was deposited (Figure 7d).

The Upper Allochthon is missing in the SW of the study area (Fig. 2), whereas it occupies the upper structural levels in the footwall of an early out-of-sequence thrust system (Figure 3; Díez Fernández et al., 2021b). This is compatible with a thrust system whose footwall wedges to the SW (Fig. 8), that is with NE-directed tectonic transport. The early out-of-sequence thrust system identified in the study area shares relative timing (post-main foliation and pre-upright folding), geometry, and kinematics with the Espiel thrust (see the description by Díez Fernández et al., 2021b). A tentative connection between the early out-of-sequence thrusts in our study area and the Espiel thrust is presented in Figure 8. Díez Fernández et al. (2021a, 2022b) suggested that these thrusts formed part of a large-scale thrust system that roots SW-wards outside the study area.

6.1.4. Late extensional tectonics

The early out-of-sequence thrust system is cut by a Variscan mafic-felsic plutonic complex (Villaviciosa – La Coronada Complex; ~345-320 Ma; Delgado-Quesada et al., 1985) (RP-11, Figure 2). This complex includes alkaline igneous rocks that were formed during a period of lithospheric extension (Sánchez Carretero et al., 1989), which also affected other sections of SW Iberia (e.g., Cambeses et al., 2015). The hanging wall rocks of the early out-of-sequence thrust system are unconformably overlain by Carboniferous syn-orogenic strata (Culm facies rock series, C1, Figure 2 and 7d), which alternate with layers of basaltic rocks (Armendariz et al., 2008). The marine sedimentation of Tournaisian to Viséan syn-orogenic strata in the study area has been ascribed to a period of crustal thinning (Armendariz et al., 2008; Martínez Poyatos, 2002; Matas et al., 2014), although no associated structure has been identified in the study area.

6.1.5. Late out-of-sequence reverse faulting and strike-slip tectonics

The related late, NE-directed, out-of-sequence reverse faults and upright folds define a breaching fault system (Figure 7d). Their geometry locally mimics the tectonic juxtaposition achieved during the early Variscan thrusting, which consists of allochthons-on-top-of-autochthon. However, these late faults are characterized by containing pieces of Carboniferous syn-orogenic strata sandwiched in between, what evidences a much longer tectonic history.

The major architecture that can be inferred for these late faults is defined by an imbricate system of SW-dipping, reverse faults that converge to a major, near vertical, sinistral fault located to the SW (see cross-sections in Figure 2). To the SW of the study area, the Azuaga Fault is a sinistral, NE-dipping, reverse fault likely formed during the same time interval (because it affects Tournaissian – Viséan strata) and is related to the same type of structures (e.g., late upright folds, sub-vertical crenulation cleavage) (Díez Fernández et al., 2021a; Díez Fernández et al., 2022b). We believe that all of these faults and associated structures define a pop-up (Figure 7d), which emerged at the center of a strike-slip system formed during transpression (Coimbra-Córdoba shear Zone; Abalos, 1990; Apalategui et al., 1990; Burg et al., 1981; Silva and Pereira, 2004) and cored by high-P rocks (Central Unit). The high vorticity associated with this positive flower structure can explain the exhumation of crust sections by extruding them from the middle-upper crust during triclinic transpression (Díez Fernández et al., 2021a; Díez Fernández et al., 2022b). This process was accommodated in part by a combination of reverse faulting and erosion (younger syn-orogenic strata lie unconformably over older ones; Apalategui et al., 1982; Díez Fernández et al., 2021b; Martínez Poyatos et al., 1998) and produced the overriding of the footwall of the early out-of-sequence thrust system onto its hanging wall.

6.2. Implications to Variscan tectonics

The basal contact of the Lower Allochthon in SW Iberia was originally a thrust, but now it is a (folded) low-angle extensional detachment around which there may be missing sections of its hanging wall and footwall. Most of the main foliation within the Lower Allochthon seems to be related to ductile flow associated with the extensional event; therefore, it is possible that some missing pieces of an early Variscan accretionary wedge on top of the Lower Allochthon (e.g., mantle wedge, ophiolites) could have been excised by similar faults. The attenuation of the Lower Allochthon by low-angle extensional faults and ductile flow before it was deformed into its current upright fold structure implies a regional shallowly dipping geometry for the Lower Allochthon after and likely before attenuation.

The Devonian suture zone represented by the Lower Allochthon is duplicated by a set of NE-directed, low-angle early thrusts, which should continue to the SW of Iberia, beyond the Central Unit. Because this thrust system transports pieces of that Devonian suture in its hanging wall, the Devonian suture must also extend to the SW of the Central Unit (Díez Fernández et al., 2016). For the same reason, the Devonian suture zone should also continue beneath the surface towards the NE, that is to reach the Central Iberian Zone.

The Coimbra-Córdoba shear zone caused extrusion and uplifting of its core along with the overlying syn-orogenic basins that covered this part of the Variscan Orogen. The current exposure of most Tournaisian – Viséan syn-orogenic deposits related to crustal extension along narrow bands cored by upright, late synforms is simply a reflection of a combination of late breaching thrusts and upright folds that disconnect the rock series that once belonged to a larger basin (see also Armendariz et al., 2008).

Variscan tectonics in this part of the orogen formed by a combination of and alternation between compressional and extensional processes that resulted in a complex structural architecture. Until recently, the role of early crustal attenuation and subhorizontal extensional flow had gone unnoticed. Also, the duplication of the suture zone containing high-P rocks and the later uplift from the middle-upper crust were not documented.

Duplication of the Devonian suture zone by out-of-sequence thrusting implies that in the absence of stratigraphic evidence, we will not be able to assess whether a piece of the suture zone is situated in the hanging wall or footwall of an out-of-sequence system fault. In an orogen like the Variscan, characterized by multiple exposures of tectonostratigraphic units that are recognized as relicts of suture zones (ophiolites, high-P rocks, and tectonic slices of the upper mantle), the occurrence of such rock assemblages may not indicate where the root zone of the suture is located. The degree of out-of-sequence thrusting has been underestimated in the Iberian Variscan Orogen. This may also be the case for other parts of the orogen. We note that some alleged Variscan suture zones may be just tectonic duplications of others.

Variscan deformation started with the subduction of the Gondwanan crust, which was followed by exhumation and structural attenuation of the existing orogenic wedge while underthrusting was still in progress. The resulting collision zone experienced further thickening by out-of-sequence thrusting, which duplicated the suture zone. Thickening was succeeded by a stage of extensional tectonics and the onset of formation of syn-orogenic basins preserved in the region. These two events were likely accompanied by prominent erosion and denudation. Resumed contraction brought about a second pulse of out-of-sequence thrusting and intracontinental strike-slip tectonics, which overprinted any previous structure, inverted previous syn-orogenic basins, and contributed to the re-thickening of the orogenic crust.

7. CONCLUSIONS

The Eastern section of the Central Unit (Eastern Ossa-Morena Complex, Iberian Massif) provides a case example for evaluating the impact of post-subduction processes on high-P rocks in their path back to the surface. Continental crust subducted during the Devonian and related to the development of a Variscan, intra-Gondwanan suture zone (Lower Allochthon), was affected by successive deformation phases, starting with its initial burial beneath the leading edge of Gondwana. Early exhumation was accompanied by progressive underthrusting of (thicker?) continental crust beneath the orogen (Autochthon), which led to attenuation, lateral flow, and exhumation of overlying and formerly accreted continental crust such as the Lower Allochthon. Further convergence led to the duplication of the Devonian suture zone by out-of-sequence thrusts directed to the Gondwana interior, seemingly blocking further accretion along the suture zone. After a transient period of extension, erosion, and basin inception, convergence was accommodated by folds and faults formed during sinistral transpression. Late faults overprinted all of the previous records and contributed to the extrusion of the underlying crust (including the high-P rocks yet to be exposed at the surface) along the cores of strike-slip shear zones (positive flower structures).

We recommend caution when dealing with exposures of suture zone-related rocks that are currently disconnected but relatively close to one another (within a few tens of kilometers). They may be part of the same major structure and are potential markers of unnoticed out-of-sequence tectonics. Late faults add to the structural complexity of collisional orogens by distorting the primary relationships between the upper and lower plates. In turn, late faults provide a geometry-based method to restore and unveil the primary geometry of suture zones, which are usually cryptic and could be lost to intense tectonic reworking in orogeny worldwide.

8. ACKNOWLEDGMENTS

This publication is part of projects PID2020-112489GB-C22 and PID2020-112489GB-C21, funded by MCIN/AEI/ 10.13039/501100011033.

9. REFERENCES CITED

Abalos, B., 1990. Cinemática y mecanismos de la deformación en régimen de transpresión. Evolución estructural y metamórfica de la Zona de Cizalla Dúctil de Badajoz-Córdoba. PhD Thesis, Universidad del País Vasco, 430 pp.

Abalos, B. and Eguiluz, L., 1989. Structural analysis of deformed early lineations in black quartzites from the Central Badajoz-Córdoba shear zone (Iberian Variscan fold belt). Revista de la Sociedad Geológica de España, 2: 95-102.

Abalos, B. and Eguiluz, L., 1990. Petrofáfrica del cuarzo en tectonitas del Corredor Blastomilinítico de Badajoz-Córdoba (SW del Macizo Ibérico). Aplicación a la cinemática de desplazamientos. Estudios Geológicos, 46: 191-208.

Abalos, B. and Eguiluz, L., 1991. Deformación transpresiva carbonífera en la Zona de Cizalla de Badajoz-Córdoba (Macizo Ibérico meridional). Revista de la Sociedad Geológica de España, 4(3-4): 229-249.

Abalos, B., Eguiluz, L. and Gil Ibarguchi, J.I., 1991a. Evolución tectono-metamórfica del Corredor Blastomilonítico de Badajoz-Córdoba. I: La Unidad Para-Autóctona. Boletín Geológico y Minero, 102-4: 491-523.

Abalos, B., Eguiluz, L. and Gil Ibarguchi, J.I., 1991b. Evolución tectono-metamórfica del Corredor Blastomilonítico de Badajoz-Córdoba. II: Las unidades alóctonas y trayectorias PTt. Boletín Geológico y Minero, 102-5: 617-671.

Abati, J., Arenas, R., Díez Fernández, R., Albert, R. and Gerdes, A., 2018. Combined zircon U-Pb and Lu-Hf isotopes study of magmatism and high-P metamorphism of the basal allochthonous units in the SW Iberian Massif (Ossa-Morena complex). Lithos, 322: 20-37.

Agard, P., Yamato, P., Jolivet, L. and Burov, E., 2009. Exhumation of oceanic blueschists and eclogites in subduction zones: Timing and mechanisms. Earth-Science Reviews, 92: 53-79.

Andreis, R.R. and Wagner, R.H., 1983. Estudio de abanicos aluviales en el norte de la cuenca Wesfaliense B de Peñarroya-Bélmez (Córdoba). In: M.J. Lemos de Sousa (Editor), Contributions to the Carboniferous Geology and Paleontology of the Iberian Peninsula. Universidade do Porto, Porto, pp. 172-227.

Apalategui, O., Borrero Domínguez, J., Delgado Quesada, M., Roldán García, F.J., Eguiluz Alarcón, L., Cueto, L.A. and Quesada, C., 1983. Mapa Geológico, Hoja

878 (Azuaga), Serie MAGNA, 1/50.000. Instituto Geológico y Minero de España.

Apalategui, O., Eguiluz, L. and Quesada, C., 1990. Ossa-Morena zone: structure. In: R.D. Dallmeyer and E. Martínez García (Editors), Pre-Mesozoic Geology of Iberia. Springer-Verlag, Berlin, Germany, pp. 280-292.

Apalategui, O., Garrote, A., Roldán García, F.J. and Sánchez Carretero, R., 1982. Mapa Geológico, Hoja 879 (Peñarroya-Pueblonuevo), Serie MAGNA, 1/50.000. Instituto Geológico y Minero de España, Madrid.

Arenas, R., Díez Fernández, R., Rubio Pascual, F.J., Sánchez Martínez, S., Martín Parra, L.M., Matas, J., González del Tánago, J., Jiménez-Díaz, A., Fuenlabrada, J.M., Andonaegui, P. and García-Casco, A., 2016. The Galicia–Ossa-Morena Zone: Proposal for a new zone of the Iberian Massif. Variscan implications. Tectonophysics, 681: 135-143.

Arenas, R., Fernández-Suárez, J., Montero, P., Díez Fernández, R., Andonaegui, P., Sánchez Martínez, S., Albert, R., Fuenlabrada, J.M., Matas, J., Martín Parra, L.M., Rubio Pascual, F.J., Jiménez-Díaz, A. and Pereira, M.F., 2018. The Calzadilla Ophiolite (SW Iberia) and the Ediacaran fore-arc evolution of the African margin of Gondwana. Gondwana Research, 58: 71-86.

Arenas, R., Novo-Fernández, I., Garcia-Casco, A., Díez Fernández, R., Fuenlabrada, J.M., Pereira, M.F., Abati, J., Sánchez Martínez, S. and Rubio Pascual, F.J., 2021. A unique blueschist facies metapelite with Mg-rich chloritoid from the Badajoz-Córdoba Unit (SW Iberian Massif): correlation of Late Devonian high-pressure belts along the Variscan Orogen. International Geology Review, 63(13): 1634-1657.

Armendariz, M., López-Guijarro, R., Quesada, C., Pin, C. and Bellido, F., 2008. Genesis and evolution of a syn-orogenic basin in transpression: Insights from petrography, geochemistry and Sm-Nd systematics in the Variscan Pedroches basin (Mississippian, SW Iberia). Tectonophysics, 461: 395-413.

Avouac, J.-P., 2003. Mountain building, erosion, and the seismic cycle in the Nepal Himalaya, Advances in Geophysics. Elsevier, pp. 1-80.

Azor, A., 1994. Evolución tectonometamórfica del límite entre las zonas Centroibérica y de Ossa-Morena (Cordillera Varisca, SO de España), Universidad de Granada, Granada, 312 pp.

Azor, A. and Ballèvre, M., 1997. Low-pressure metamorphism in the Sierra Albarrana area (Variscan Belt, Iberian Massif). Journal of Petrology, 38: 35-64.

Azor, A., Lodeiro, F.G. and Simancas, J.F., 1994. Tectonic evolution of the boundary between the Central Iberian and Ossa-Morena zones (Variscan belt, southwest Spain). Tectonics, 13: 45-61.

Azor, A., Simancas, J., Martínez Potayos, D., Montero, P., González Lodeiro, F. and Pérez-Cáceres, I., 2016. U-Pb zircon age and tectonic meaning of the Cardenchosa pluton (Ossa-Morena Zone). Geo-Temas (IX Congreso Geológico de España), 16(2): 23-26.

Azor, A., Simancas, J.F., Martínez Poyatos, D.J., Montero, P., Bea, F., González Lodeiro, F. and Gabites, J., 2012. Nuevos datos geocronológicos sobre la evolución tectonometamórfica de la Unidad de Sierra Albarrana (Zona de Ossa-Morena, SO de Iberia). Geotemas, 13: 341-344.

Burg, J.P., Iglesias, M., Laurent, P., Matte, P. and Ribeiro, A., 1981. Variscan intracontinental deformation: the Coimbra-Cordoba shear zone (SW Iberian Peninsula). Tectonophysics, 78: 161-177.

Cambeses, A., Scarrow, J.H., Montero, P., Molina, J.F. and Moreno, J.A., 2015. SHRIMP U–Pb zircon dating of the Valencia del Ventoso plutonic complex, Ossa-Morena Zone, SW Iberia: Early Carboniferous intra-orogenic extension-related 'calc-alkaline' magmatism. Gondwana Research, 28(2): 735-756.

Cardozo, N. and Allmendinger, R.W., 2013. Spherical projections with OSXStereonet. Computers & Geosciences, 51(0): 193 - 205.

Dallmeyer, R.D. and Quesada, C., 1992. Cadomian vs. Variscan evolution of the Ossa-Morena zone (SW Iberia): field and ^{40}Ar/^{39}Ar mineral age constraints. Tectonophysics, 216: 339-364.

Delgado Quesada, M., 1971. Esquema Geológico de la hoja No. 878 de Azuaga (Badajoz). Boletín Geológico Minero, 82: 277-286.

Delgado-Quesada, M., Garrote, A., and Sánchez-Carretero, R., 1985. El magmatismo de la Alineación La Coronada-Villaviciosa de Córdoba en su mitad oriental, Zona de Ossa-Morena. Temas Geológico Mineros, 7 (5ª Reunión del G.O.M.), 41-64.

Dewey, J.F., 1988. Extensional collapse of orogens. Tectonics, 7: 1123-1139.

Dias da Silva, Í., Pereira, M. F., Silva, J. B. and Gama, C., 2018. Time-space distribution of silicic plutonism in a gneiss dome of the Iberian Variscan Belt: The Évora Massif (Ossa-Morena Zone, Portugal). Tectonophysics, 747-748: 298-317.

Díez Fernández, R. and Arenas, R., 2015. The Late Devonian Variscan suture of the Iberian Massif: A correlation of high-pressure belts in NW and SW Iberia. Tectonophysics, 654: 96-100.

Díez Fernández, R. and Arenas, R., 2016. Reply to Comment on "The Late Devonian Variscan suture of the Iberian Massif: A correlation of high-pressure belts in NW and SW Iberia". Tectonophysics, 670: 155-160.

Díez Fernández, R., Arenas, R., Pereira, M.F., Sánchez Martínez, S., Albert, R., Martín Parra, L.M., Rubio Pascual, F.J. and Matas, J., 2016. Tectonic evolution of Variscan Iberia: Gondwana - Laurussia collision revisited. Earth-Science Reviews, 162: 269-292.

Díez Fernández, R., Arenas, R., Rojo-Pérez, E., Sánchez Martínez, S. and Fuenlabrada, J.M., 2022a. Tectonostratigraphy of the Mérida Massif reveals a new Cadomian suture zone exposure in Gondwana (SW Iberia). International Geology Review, 64(3): 405-424.

Díez Fernández, R., Fernández, C., Arenas, R. and Novo-Fernández, I., 2021a. On the Rootless Nature of a Devonian Suture in SW Iberia (Ossa-Morena Complex, Variscan Orogen): Geometry and Kinematics of the Azuaga Fault. Tectonics, 40(6): e2021TC006791.

Díez Fernández, R., Fernández, C., Arenas, R. and Novo-Fernández, I., 2022b. Reply to Comment by Azor et al. on "On the Rootless Nature of a Devonian Suture in SW Iberia (Ossa-Morena Complex, Variscan Orogen): Geometry and Kinematics of the Azuaga Fault". Tectonics, 41(1): e2021TC007154.

Díez Fernández, R., Jiménez-Díaz, A., Arenas, R., Pereira, M.F. and Fernández-Suárez, J., 2019. Ediacaran Obduction of a Fore-arc Ophiolite in SW Iberia: A Turning Point in the Evolving Geodynamic Setting of Peri-Gondwana. Tectonics, 38: 95-119.

Díez Fernández, R. and Martínez Catalán, J.R., 2012. Stretching lineations in high-pressure belts: the fingerprint of subduction and subsequent events (Malpica–Tui complex, NW Iberia). Journal of the Geological Society, 169: 531-543.

Díez Fernández, R., Martínez Catalán, J.R., Arenas, R. and Abati, J., 2011. Tectonic evolution of a continental subduction-exhumation channel: Variscan structure of the basal allochthonous units in NW Spain. Tectonics, 30: TC3009.

Díez Fernández, R., Martínez Catalán, J.R., Gómez Barreiro, J. and Arenas, R., 2012. Extensional flow during gravitational collapse: a tool for setting plate convergence (Padrón migmatitic dome, Variscan belt, NW Iberia). The Journal of Geology, 120: 83-103.

Díez Fernández, R., Matas, J., Arenas, R., Martín-Parra, L.M., Sánchez Martínez, S., Novo-Fernández, I. and Rojo-Pérez, E., 2021b. Two-step obduction of the Porvenir Serpentinite: a cryptic Devonian suture in SW Iberian Massif (Ossa-Morena Complex). In: J. Wakabayashi and Y. Dilek (Editors), Plate Tectonics, Ophiolites, and Societal Significance of Geology: A Celebration of the Career of Eldridge Moores. GSA Books, pp. 113-132.

Eguíluz, L., Gil Ibarguchi, J.I., Abalos, B. and Apraiz, A., 2000. Superposed Hercynian and Cadomian orogenic cycles in the Ossa-Morena zone and related areas of the Iberian Massif. Geological Society of America Bulletin, 112: 1398-1413.

Ernst, W.G. and Liou, J.G., 2008. High- and ultrahigh-pressure metamorphism: Past results and future prospects. American Mineralogist, 93: 1771-1786.

Expósito, I., Simancas, J.F., González Lodeiro, F., Azor, A. and Martínez Poyatos, D.J., 2002. La estructura de la mitad septentrional de la Zona de Ossa-Morena: deformación en el bloque inferior de un cabalgamiento cortical de evolución compleja. Revista de la Sociedad Geológica de España, 15: 3-14.

Expósito, I., Simancas, J.F., González Lodeiro, F., Bea, F., Montero, P. and Salman, K., 2003. Metamorphic and deformational imprint of Cambrian-Lower Ordovician rifting in the Ossa-Morena Zone (Iberian Massif, Spain). Journal of Structural Geology, 25: 2077-2087.

Fuenlabrada, J.M., Arenas, R., Díez Fernández, R., González del Tánago, J., Martín-Parra, L.M., Matas, J., Rojo-Pérez, E., Sánchez Martínez, S., Andonaegui, P. and Solis Alulima, B., 2021. Tectonic setting and isotopic sources (Sm–Nd) of the SW Iberian Autochthon (Variscan Orogen). Journal of Iberian Geology, 47: 121-150.

García Casquero, J.L., Priem, H.N.A., Boelrijk, N.A.I.M. and Chacon, J., 1988. Isotopic dating of the mylonitization of the Azuaga Group in the Badajóz-Córdoba belt, SW Spain. Geologische Rundschau, 77: 483-489.

Gerya, T.V., Perchuk, L.L. and Burg, J.-P., 2008. Transient hot channels: Perpetrating and regurgitating ultrahigh-pressure, high-temperature crust–mantle associations in collision belts. Lithos, 103(1-2): 236-256.

Gerya, T.V., Stöckhert, B. and Perchuk, A., 2002. Exhumation of high-pressure metamorphic rocks in a subduction channel: A numerical simulation. Tectonics, 21: 1056.

González del Tánago, J. and Arenas, R., 1991. Anfibolitas granatíferas de Sierra Albarrana, Córdoba : termobarometría e implicaciones para el desarrollo del metamorfismo regional. Revista de la Sociedad Geológica de España, 4: 251-269.

Guillot, S., Hattori, K., Agard, P., Schwartz, S. and Vidal, O., 2009. Exhumation Processes in Oceanic and Continental Subduction Contexts: A Review. In: Subduction Zone Geodynamics (Lallemand, S. and Funiciello, F., Eds). Frontiers in Earth Sciences: 175-205.

Jensen, S., Palacios, T. and Eguiluz, L., 2004. Cambrian ichnofabrics from the Ossa Morena and Central Iberian zones: preliminary results. Geo-Temas, 6(2): 291-293.

Jolivet, L., Faccenna, C., Goffé, B., Burov, E. and Agard, P., 2003. Subduction tectonics and exhumation of high-pressure metamorphic rocks in the Mediterranean orogens. American Journal of Science, 303: 353-409.

Kroner, U. and Romer, R.L., 2013. Two plates — Many subduction zones: The Variscan orogeny reconsidered. Gondwana Research, 24: 298-329.

Liñán, E., 1978. Bioestratigrafía de la Sierra de Córdoba. PhD Thesis, Universidad de Granada, Granada, 212 pp.

Little, T.A., Hacker, B.R., Gordon, S.M., Baldwin, S.L., Fitzgerald, P.G., Ellis, S. and Korchinski, M., 2011. Diapiric exhumation of Earth's youngest (UHP) eclogites in the gneiss domes of the D'Entrecasteaux Islands, Papua New Guinea. Tectonophysics, 510(1): 39-68.

López Sánchez-Vizcaíno, V., Gómez-Pugnaire, M.T., Azor, A. and Fernández-Soler, J.M., 2003. Phase diagram sections applied to amphibolites: a case study from the Ossa-Morena/Central Iberian Variscan suture (Southwestern Iberian Massif). Lithos, 68(1): 1-21.

Maierová, P., Schulmann, K., Štípská, P., Gerya, T. and Lexa, O., 2021. Trans-lithospheric diapirism explains the presence of ultra-high pressure rocks in the European Variscides. Communications Earth & Environment, 2(1): 56.

Malusà, M.G., Faccenna, C., Baldwin, S.L., Fitzgerald, P.G., Rossetti, F., Balestrieri, M.L., Danišík, M., Ellero, A., Ottria, G., and Piromallo, C., 2015. Contrasting styles of (U)HP rock exhumation along the Cenozoic Adria-Europe plate

boundary (Western Alps, Calabria, Corsica). Geochemistry, Geophysics, Geosystems, 16(6): 1786-1824.
Martínez Poyatos, D., González Lodeiro, F., Azor, A. and Simancas, J.F., 2001. La estructura de la Zona Centroibérica en la región de Los Pedroches (Macizo Ibérico meridional). Revista de la Sociedad Geológica de España, 14: 147-160.
Martínez Poyatos, D., Simancas, J.F., Azor, A. and González Lodeiro, F., 1998. Evolution of a Carboniferous piggyback basin in the southern Central Iberian Zone (Variscan Belt, SE Spain). Bulletin de la Société Geologique de France, 169: 573-578.
Martínez Poyatos, D.J., 2002. Estructura del borde meridional de la Zona Centroibérica y su relación con el contacto entre las Zonas Centroibérica y de Ossa-Morena. Nova Terra, 18: 1-295.
Matas, J., Martín Parra, L. and Montes Santiago, M., 2014. Un olistostroma con cantos y bloques del Paleozoico Inferior en la cuenca carbonífera del Guadalmellato (Córdoba). Parte I: Estratigrafía y marco geodinámico varisco. Revista de la Sociedad Geológica de España, 27(1): 11-26.
Matas, J., Martín Parra, L.M. and Martínez Poyatos, D., 2015. Mapa y Memoria del Mapa Geológico Nacional a escala 1:200.000 (MAGE200) nº 69 (Pozoblanco). Instituto Geológico y Minero de España.
Matte, P., 2001. The Variscan collage and orogeny (480-290 Ma) and the tectonic definition of the Armorica microplate: a review. Terra Nova, 13: 122-128.
Novo-Fernández, I., Arenas, R., de Capitani, C., Pereira, M.F., Díez Fernández, R., Sánchez Martínez, S. and Garcia-Casco, A., 2021. Tracking the late Devonian high-P metamorphic belt in the Variscan Orogen: New constraints on the PT

evolution of eclogites from the Cubito-Moura Unit (SW Iberian Massif). Lithos, 386-387: 106015.

Ordóñez Casado, B., 1998. Geochronological studies of the Pre-Mesozoic basement of the Iberian Massif: the Ossa Morena zone and the Allochthonous Complexes within the Central Iberian zone. PhD Thesis, Swiss Federal Institute of Technology, Zürich, Switzerland, 235 pp.

Ortuño, M.G., 1971. Middle Westphalian strata in South-West Spain. Proceedings of the VII Congr. Intern. Strat. Géol. Carbonif. (Shejfield, 1967), 3: 1275-1292.

Passchier, C. W., 1997. The fabric attractor. Journal of Structural Geology, 19: 113-127.

Pavlis, T.L., Picornell, C., Serpa, L., Bruhn, R.L. and Plafker, G., 2004. Tectonic processes during oblique collision: Insights from the St. Elias orogen, northern North American Cordillera. Tectonics, 23(3).

Pereira, M.F., Apraiz, A., Chichorro, M., Silva, J.B. and Armstrong, R.A., 2010a. Exhumation of high-pressure rocks in northern Gondwana during the Early Carboniferours (Coimbra-Cordoba shear zone, SW Iberian Massif): Tectonothermal analysis and U–Th–Pb SHRIMP in-situ zircon geochronology. Gondwana Research, 17: 440-460.

Pereira, M.F., Chichorro, M., Silva, J.B., Ordóñez-Casado, B., Lee, J.K.W. and Williams, I.S., 2012. Early Carboniferous wrenching, exhumation of high-grade metamorphic rocks and basin instability in SW Iberia: Constraints derived from structural geology and U–Pb and ^{40}Ar–^{39}Ar geochronology. Tectonophysics, 558-559: 28-44.

Pereira, M.F., Chichorro, M., Williams, I.S., Silva, J.B., Fernández, C., Díaz-Azpíroz, M., Apraiz, A. and Castro, A., 2009. Variscan intra-orogenic extensional tectonics in the Ossa-Morena Zone (Évora-Aracena-Lora del Río metamorphic

belt, SW Iberian Massif): SHRIMP zircon U–Th–Pb geochronology. Geological Society, London, Special Publications, 327: 215-237.
Pereira, M.F., Silva, J.B., Drost, K., Chichorro, M. and Apraiz, A., 2010b. Relative timing of transcurrent displacements in northern Gondwana: U–Pb laser ablation ICP-MS zircon and monazite geochronology of gneisses and sheared granites from the western Iberian Massif (Portugal). Gondwana Research, 17: 461-481.
Platt, J.P., 1993. Exhumation of high-pressure rocks: a review of concepts and processes. Terra Nova, 5(2): 119-133.
Quesada, C., 1990. Precambrian successions in SW Iberia: their relationship to 'Cadomian' orogenic events. In: D.R. Lemos, R.A. Strachan and C.G. Topley (Editors), The Cadomian Orogeny. Geological Society, London, Special Publication. Geological Society, London, Special Publication, pp. 353-362.
Quesada, C. and Dallmeyer, R.D., 1994. Tectonothermal evolution of the Badajoz-Cordoba shear zone (SW Iberia): characteristics and $^{40}Ar/^{39}Ar$ mineral age constraints. Tectonophysics, 231: 195-213.
Rey, P., Vanderhaeghe, O. and Teyssier, C., 2001. Gravitational collapse of the continental crust: definition, regimes and modes. Tectonophysics, 342: 435-449.
Rojo-Pérez, E., Linnemann, U., Hofmann, M., Fuenlabrada, J.M., Zieger, J., Fernández-Suárez, J., Andonaegui, P., Sánchez Martínez, S., Díez Fernández, R. and Arenas, R., 2022. U-Pb geochronology and isotopic geochemistry of adakites and related magmas in the Ediacaran arc section of the SW Iberian Massif: The role of subduction erosion cycles in peri-Gondwanan arcs. Gondwana Research, 109: 89-112.
Sánchez Carretero, R., Carracedo, M., Gil Ibarguchi, J.I. and Ortega Cuesta, L., 1989. Unidades y datos geoquímicos del magmatismo Hercínico de la "Alineación de

Villaviciosa de Córdoba - La Coronada" (Ossa Morena Oriental). Studia Geologica Salmanticensia, vol. especial 4: 107-131.

Schäfer, H.J., Gebauer, D. and Nägler, T.F., 1991. Evidence for Silurian eclogite and granulite facies metamorphism in the Badajoz-Córdoba Shear belt, SW Spain. Terra Nova, 3, suppl. 6: 11.

Schulmann, K., Lexa, O., Janoušek, V., Lardeaux, J.M. and Edel, J.B., 2014. Anatomy of a diffuse cryptic suture zone: An example from the Bohemian Massif, European Variscides. Geology, 42(4): 275-278.

Shelley, D. and Bossière, G., 2000. A new model for the Hercynian Orogen of Gondwanan France and Iberia. Journal of Structural Geology, 22: 757-776.

Silva, J.B. and Pereira, M.F., 2004. Transcurrent continental tectonics model for the Ossa-Morena Zone Neoproterozoic-Paleozoic evolution, SW Iberian Massif, Portugal. International Journal of Earth Sciences, 93: 886-896.

Simancas, J.F., Azor, A., Martínez-Poyatos, D., Tahiri, A., El Hadi, H., González-Lodeiro, F., Pérez-Estaún, A. and Carbonell, R., 2009. Tectonic relationships of Southwest Iberia with the allochthons of Northwest Iberia and the Moroccan Variscides. Comptes Rendus Geoscience, 341: 103-113.

Solá, A.R., Williams, I.S., Neiva, A.M.R. and Ribeiro, M.L., 2009. U–Th–Pb SHRIMP ages and oxygen isotope composition of zircon from two contrasting late Variscan granitoids, Nisa-Albuquerque batholith, SW Iberian Massif: Petrologic and regional implications. Lithos, 111: 156-167.

Solís-Alulima, B., Abati, J., López-Carmona, A., Gutiérrez-Alonso, G., Fernández-Suárez, J. and Stockli, D.F., 2022. Detrital zircon ages and provenance of a Cambrian succession in the Sierra Albarrana Domain (SW Iberian Massif). Lithos, 408-409: 106542.

Solís-Alulima, B., López-Carmona, A. and Abati, J., 2020. Ordovician metamorphism and magmatism preserved in the Ossa Morena Complex: SHRIMP geochronology, geochemistry and Sr-Nd isotopic signatures of the Sierra Albarrana Domain (SW Iberian Massif). Lithos, 374-375: 105700.

Strak, V., Dominguez, S., Petit, C., Meyer, B. and Loget, N., 2011. Interaction between normal fault slip and erosion on relief evolution: Insights from experimental modelling. Tectonophysics, 513(1): 1-19.

Vanderhaeghe, O., 2012. The thermal-mechanical evolution of crustal orogenic belts at convergent plate boundaries: a reappraisal of the orogenic cycle. Journal of Geodynamics, 56-57: 124-145.

Wagner, R.H., 2004. The Iberian Massif: a Carboniferous assembly. Journal of Iberian Geology, 30: 93-108.

Warren, C.J., 2013. Exhumation of (ultra-)high-pressure terranes: concepts and mechanisms. Solid Earth, 4: 75-92.

Willner, A.P., Sebazungu, E., Gerya, T.V., Maresch, W.V. and Krohe, A., 2002. Numerical modelling of PT-paths related to rapid exhumation of high-pressure rocks from the crustal root in the Variscan Erzgebirge Dome (Saxony/Germany). Journal of Geodynamics, 33: 281-314.

Woodcock, N.H. and Daly, M.C., 1986. The Role of Strike-Slip Fault Systems at Plate Boundaries [and Discussion]. Philosophical Transactions of the Royal Society of London. Series A, Mathematical and Physical Sciences, 317(1539): 13-29.

Yamato, P., Agard, P., Burov, E., Le Pourhiet, L., Jolivet, L. and Tiberi, C., 2007. Burial and exhumation in a subduction wedge: Mutual constraints from thermomechanical modeling and natural P-T-t data (Schistes Lustres, western Alps). Journal of Geophysical Research-Solid Earth, 112.

FIGURE CAPTION

Figure 1: (a) Tectonic sketch of the Variscan orogen and (b) geological map of the Iberian Massif indicating the main terranes involved in the orogeny (Díez Fernández and Arenas, 2015). (c) Location of the study areas on a regional map of SW Iberian Massif (Díez Fernández et al., 2021a). Abbreviations: AF — Azuaga Fault; BToIP — Basal Thrust of the Iberian Parautochthon; BAO — Beja–Acebuches Ophiolite; CA — Carvalhal Amphibolites; CF — Canaleja Fault; CMU — Cubito–Moura Unit; CO — Calzadilla Ophiolite; CU — Central Unit; EsT — Espiel Thrust; EU—Escoural Unit; ET—Espina Thrust; HF— Hornachos Fault; IOMZO —Internal Ossa-Morena Zone Ophiolites; J–PCSZ — Juzbado-Penalva do Castelo Shear Zone; LFT — Lalín-Forcarei Thrust; LPSZ — Los Pedroches Shear Zone; LLSZ — Llanos Shear Zone; MLSZ — Malpica–Lamego Shear Zone; MF — Matachel Fault; OF — Onza Fault; OVD — Obejo–Valsequillo Domain; PG–CVD — Puente Génave–Castelo de Vide Detachment; PRSZ— Palas de Rei Shear Zone; PTSZ — Porto–Tomar Shear Zone; RF — Riás Fault; SISZ —South Iberian Shear Zone; VF — Viveiro Fault; ZSI — Zalamea de la Serena Imbricates.

Figure 2: Geological map and cross-sections of the eastern part of the Central Unit and its surrounding terranes (location in Figure 1). Data to constrain the age and in-depth descriptions of the lithostratigraphic assemblages can be found in published works (Delgado Quesada, 1971; Ortuño, 1971; Liñán, 1978; Apalategui et al., 1982, 1983; Andreis and Wagner, 1983; Delgado-Quesada et al., 1985; Sánchez Carretero et al., 1989; Abalos, 1990; Azor, 1994; Azor et al., 1994; Azor and Ballèvre, 1997; Martínez Poyatos,

2002; Jensen et al., 2004; Pereira et al., 2010a; Matas et al., 2015; Abati et al., 2018; Fuenlabrada et al., 2021).

Figure 3: (a) Geological map and (b and c) cross-sections of the northeastern part of the Ossa-Morena Complex, to the north of the study area shown in Figure 2 (location in Figure 1) (Díez Fernández et al., 2021b).

Figure 4: (a) Main foliation in schists of the Albariza-Bembézar Succession affected by NE-verging upright folds. Note the orientation of late crenulation cleavage (red dashed line). (b) Late crenulation cleavage (red dashed line) affecting bedding (yellow dashed line) in phyllites of the Azuaga Formation. (c) Asymmetric, isoclinal recumbent folds in meta-sandstones from the Albariza-Bembézar Succession. The bedding is marked by yellow dashed lines, and the (main) axial plane foliation is green. (d) NE-verging, asymmetric, upright folds affecting the main foliation of migmatitic paragneisses from the Central Unit. (e) Main foliation and associated stretching lineation in paragneisses from the Central Unit. (f) Mylonitic foliation in albite-bearing paragneisses from the Central Unit. Note the top-to-the-SE C-S structures defined by C-planes (green dashed line) and S-planes (white dashed lines). (g) Recumbent isoclinal folds formed in gneisses from the Central Unit (main foliation is axial-planar). Note that pronounced stretching along the forelimbs and sigma-shaped quartz segregates, indicating top-to-the-SE shearing. (h) Main foliation in felsic orthogneisses from the Central Unit with sigma-shaped quartz and feldspar porphyroclasts, indicating top-to-the-SE shearing.

Figure 5: Lower hemisphere equal area projections showing the orientation of the lineation in the Autochthon and Lower Allochthon. (a) Stretching lineation related to the

main foliation in the Autochthon. (b) Intersection lineation (bedding and main foliation) in the Autochthon. (c) Crenulation lineation related to the main foliation in the Autochthon. (d) Stretching and (e) mineral lineation related to the main foliation in the Lower Allochthon. (f) Stereoplot including all lineations and showing a possible path of counter-clockwise reorientation to fabric attractors (axial planes and fold axis) calculated in Figure 6.

Figure 6: Stereoplots showing the orientation of the main planar microstructures in the Autochthon, syn-orogenic strata, and Lower Allochthon. The plots include the pi-axes and axial planes of the upright folds, which they collectively define. (a) Plot including late crenulation cleavage together with the calculated axial planes and fold axes (see the following sections). (b) Bedding in the Autochthon. (c) Bedding in the syn-orogenic strata. (d) Main foliation in the Autochthon. (e) Main foliation in the Lower Allochthon.

Figure 7: Simplified tectonic model explaining the exhumation of high-P rocks related to a (a) suture zone that is (b) constricted and attenuated after accretion and then (c) affected by early out-of-sequence thrusting, followed by (d) erosion and inception of a syn-orogenic basin. Further contraction resulted in late out-of-sequence reverse faulting and upright folding (Figure 8). White stars represent visual references at the same location throughout each step of the model.

Figure 8: (a) Composite cross-section, including section E-E’ from Figure 2 and section B-B’ from Figure 3. (b) Integration of lithological units into broader tectonic units that discriminates a lower plate (Autochthon *s.l.*) and a Devonian suture zone (Lower Allochthon and lenses of mantle rocks, such as meta-peridotites) from an upper plate

(Upper Allochthon *s.l.*). Syn-orogenic strata are omitted for simplicity and better visualization of the thrust nappes. The legend follows Figure 7 and results from the gathering of units shown via boxes and arrows. The primary and secondary contacts shown in section (a) are kept in (b) to track the units between the cross-sections.

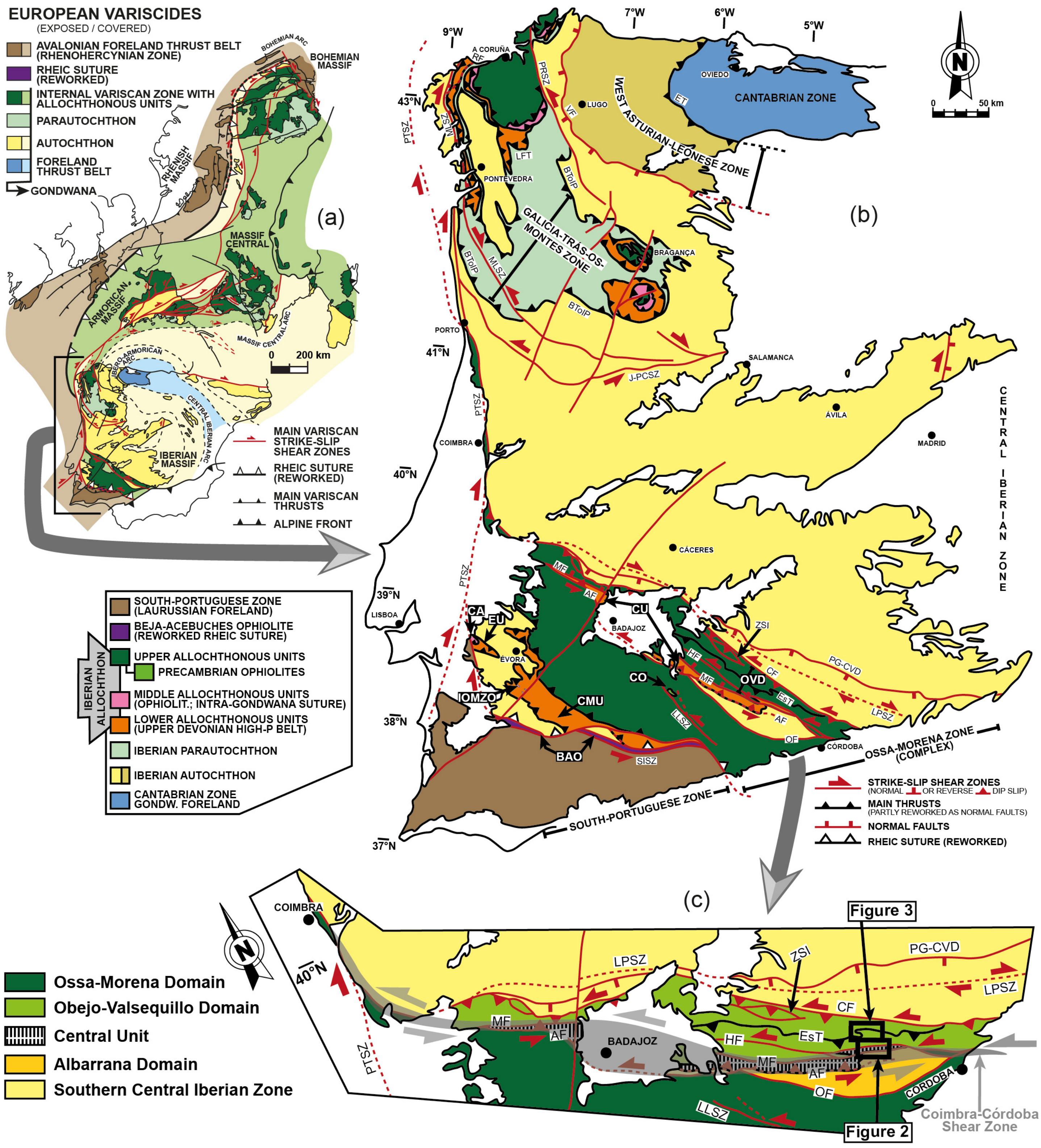

EUROPEAN VARISCIDES
(EXPOSED / COVERED)
AVALONIAN FORELAND THRUST BELT (RHENOHERCYNIAN ZONE)
RHEIC SUTURE (REWORKED)
INTERNAL VARISCAN ZONE WITH ALLOCHTHONOUS UNITS
PARAUTOCHTHON
AUTOCHTHON
FORELAND THRUST BELT
GONDWANA
(a)
BOHEMIAN ARC
BOHEMIAN MASSIF
RHENISH MASSIF
MASSIF CENTRAL
ARMORICAN MASSIF
MASSIF CENTRAL ARC
IBERO-ARMORICAN ARC
CENTRAL IBERIAN ARC
IBERIAN MASSIF
0 200 km
MAIN VARISCAN STRIKE-SLIP SHEAR ZONES
RHEIC SUTURE (REWORKED)
MAIN VARISCAN THRUSTS
ALPINE FRONT
(b)
9°W
7°W
6°W
5°W
43°N
41°N
40°N
39°N
38°N
37°N
0 50 km
N
A CORUÑA
RF
LUGO
OVIEDO
ET
CANTABRIAN ZONE
WEST ASTURIAN-LEONESE ZONE
PRSZ
VF
MLSZ
PTSZ
LFT
PONTEVEDRA
BToIP
GALICIA-TRÁS-OS-MONTES ZONE
BRAGANÇA
PORTO
SALAMANCA
J-PCSZ
ÁVILA
MADRID
COIMBRA
CENTRAL IBERIAN ZONE
CÁCERES
MF
AF
CU
CA
EU
LISBOA
BADAJOZ
ZSI
HF
CF
PG-CVD
ÉVORA
CO
OVD
EsT
LPSZ
IOMZO
CMU
LLSZ
OF
CÓRDOBA
BAO
SISZ
OSSA-MORENA ZONE (COMPLEX)
SOUTH-PORTUGUESE ZONE
SOUTH-PORTUGUESE ZONE (LAURUSSIAN FORELAND)
BEJA-ACEBUCHES OPHIOLITE (REWORKED RHEIC SUTURE)
UPPER ALLOCHTHONOUS UNITS
PRECAMBRIAN OPHIOLITES
MIDDLE ALLOCHTHONOUS UNITS (OPHIOLIT.; INTRA-GONDWANA SUTURE)
LOWER ALLOCHTHONOUS UNITS (UPPER DEVONIAN HIGH-P BELT)
IBERIAN PARAUTOCHTHON
IBERIAN AUTOCHTHON
CANTABRIAN ZONE GONDW. FORELAND
IBERIAN ALLOCHTHON
STRIKE-SLIP SHEAR ZONES (NORMAL OR REVERSE DIP SLIP)
MAIN THRUSTS (PARTLY REWORKED AS NORMAL FAULTS)
NORMAL FAULTS
RHEIC SUTURE (REWORKED)
(c)
Figure 3
Figure 2
COIMBRA
40°N
PTSZ
LPSZ
ZSI
PG-CVD
CF
MF
AF
BADAJOZ
HF
EsT
OF
LLSZ
CORDOBA
Coimbra-Córdoba Shear Zone
Ossa-Morena Domain
Obejo-Valsequillo Domain
Central Unit
Albarrana Domain
Southern Central Iberian Zone

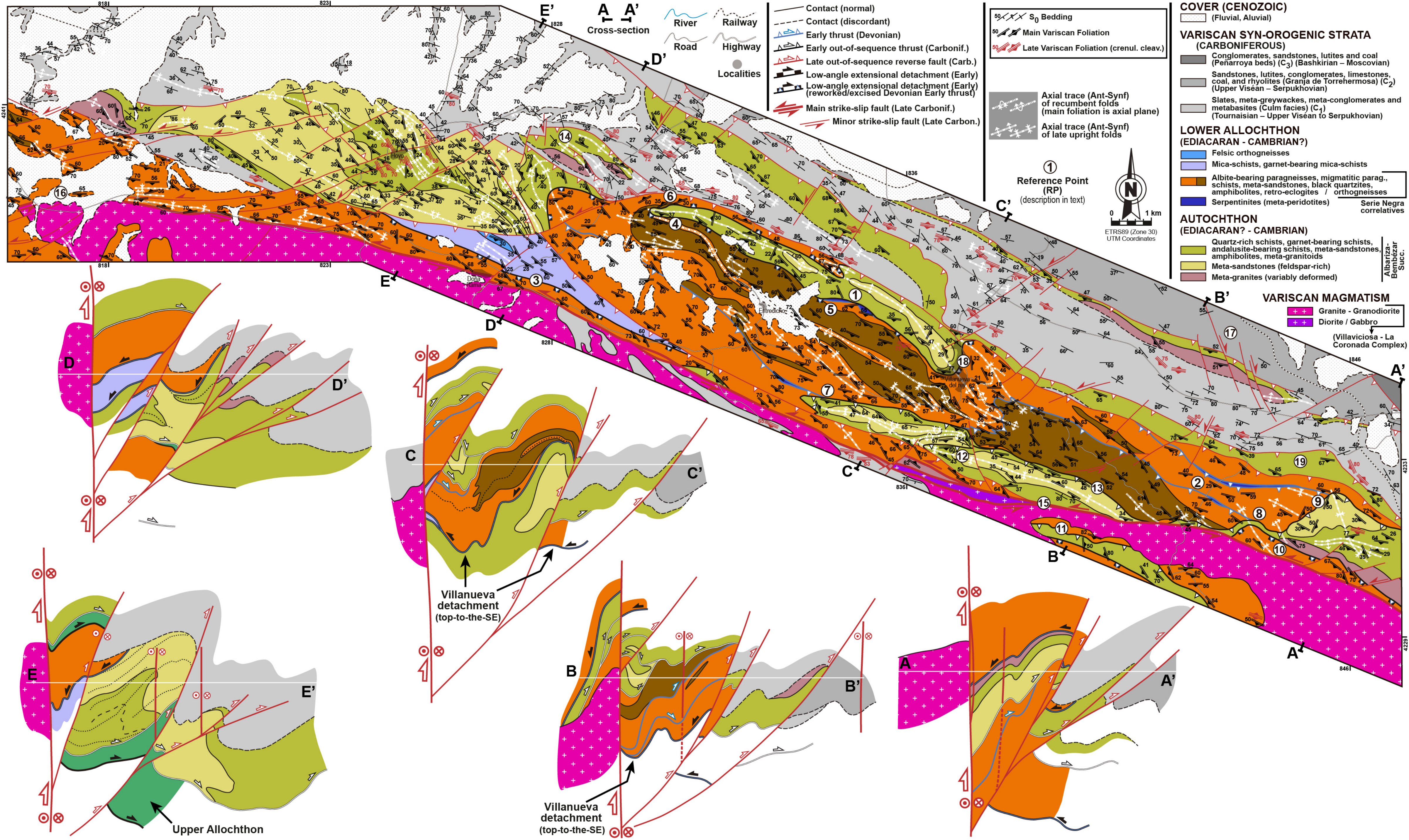

Cross-section
River
Railway
Road
Highway
Localities
Contact (normal)
Contact (discordant)
Early thrust (Devonian)
Early out-of-sequence thrust (Carbonif.)
Late out-of-sequence reverse fault (Carb.)
Low-angle extensional detachment (Early)
Low-angle extensional detachment (Early) (reworked/excised Devonian Early thrust)
Main strike-slip fault (Late Carbonif.)
Minor strike-slip fault (Late Carbon.)
S0 Bedding
Main Variscan Foliation
Late Variscan Foliation (crenul. cleav.)
Axial trace (Ant-Synf) of recumbent folds (main foliation is axial plane)
Axial trace (Ant-Synf) of late upright folds
Reference Point (RP) (description in text)
ETRS89 (Zone 30) UTM Coordinates
COVER (CENOZOIC)
(Fluvial, Aluvial)
VARISCAN SYN-OROGENIC STRATA (CARBONIFEROUS)
Conglomerates, sandstones, lutites and coal (Peñarroya beds) (C3) (Bashkirian – Moscovian)
Sandstones, lutites, conglomerates, limestones, coal, and rhyolites (Granja de Torrehermosa) (C2) (Upper Viséan – Serpukhovian)
Slates, meta-greywackes, meta-conglomerates and metabasites (Culm facies) (C1) (Tournaisian – Upper Viséan to Serpukhovian)
LOWER ALLOCHTHON (EDIACARAN - CAMBRIAN?)
Felsic orthogneisses
Mica-schists, garnet-bearing mica-schists
Albite-bearing paragneisses, migmatitic parag., schists, meta-sandstones, black quartzites, amphibolites, retro-eclogites / orthogneisses
Serpentinites (meta-peridotites)
Serie Negra correlatives
AUTOCHTHON (EDIACARAN? - CAMBRIAN)
Quartz-rich schists, garnet-bearing schists, andalusite-bearing schists, meta-sandstones, amphibolites, meta-granitoids
Meta-sandstones (feldspar-rich)
Meta-granites (variably deformed)
Albariza-Bembézar Succ.
VARISCAN MAGMATISM
Granite - Granodiorite
Diorite / Gabbro
(Villaviciosa - La Coronada Complex)
Hoyo
Doña Rama
Entredicho
Villanueva del rey
D D'
C C'
E E'
B B'
A A'
Villanueva detachment (top-to-the-SE)
Villanueva detachment (top-to-the-SE)
Upper Allochthon

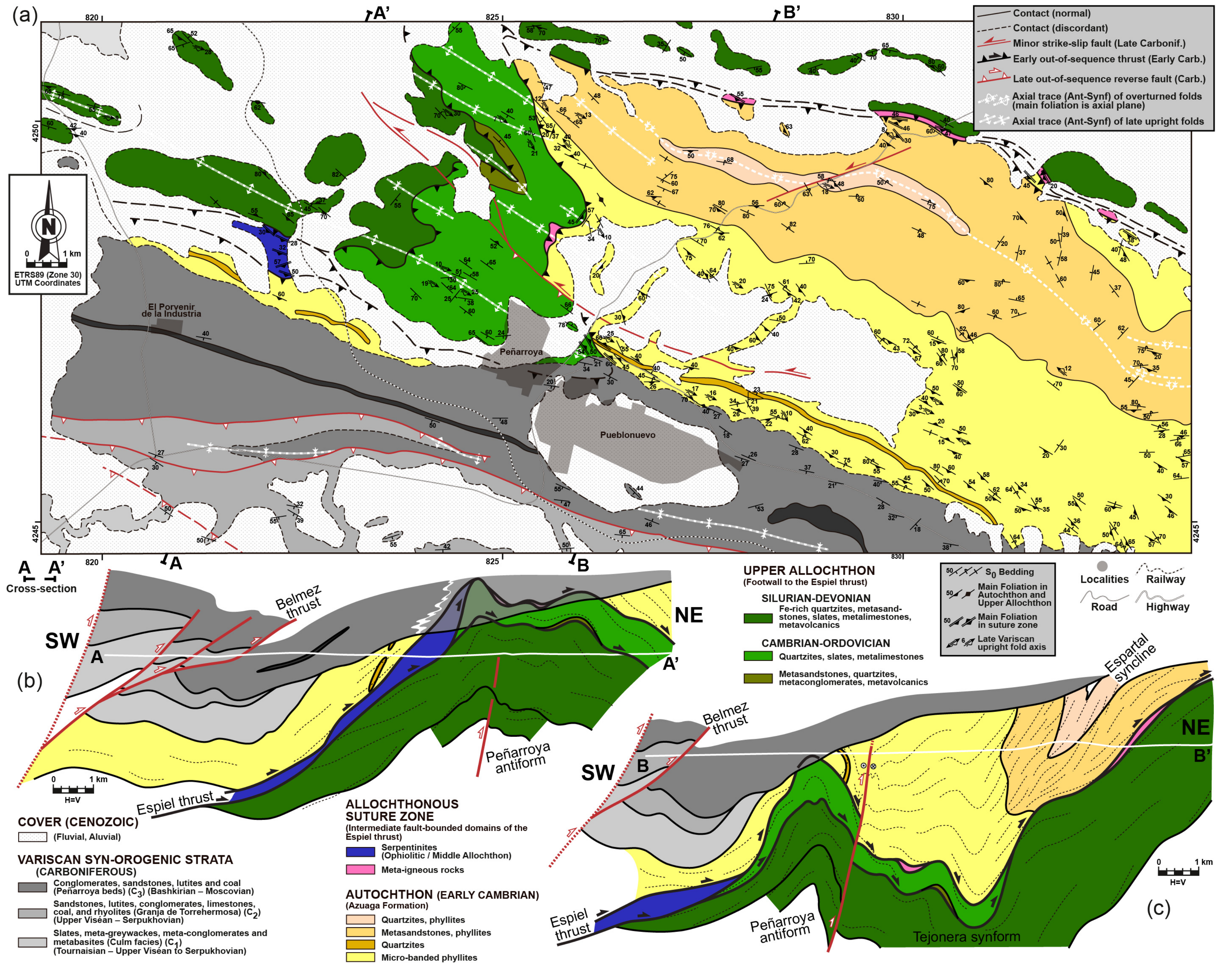
(a)
A'
B'
820
825
830
4250
4245
Contact (normal)
Contact (discordant)
Minor strike-slip fault (Late Carbonif.)
Early out-of-sequence thrust (Early Carb.)
Late out-of-sequence reverse fault (Carb.)
Axial trace (Ant-Synf) of overturned folds (main foliation is axial plane)
Axial trace (Ant-Synf) of late upright folds
N
0 1 km
ETRS89 (Zone 30) UTM Coordinates
El Porvenir de la Industria
Peñarroya
Pueblonuevo
A
B
A A' Cross-section
SW
NE
Belmez thrust
(b)
Peñarroya antiform
Espiel thrust
0 1 km H=V
UPPER ALLOCHTHON
(Footwall to the Espiel thrust)
SILURIAN-DEVONIAN
Fe-rich quartzites, metasandstones, slates, metalimestones, metavolcanics
CAMBRIAN-ORDOVICIAN
Quartzites, slates, metalimestones
Metasandstones, quartzites, metaconglomerates, metavolcanics
S_0 Bedding
Main Foliation in Autochthon and Upper Allochthon
Main Foliation in suture zone
Late Variscan upright fold axis
Localities
Railway
Road
Highway
Espartal syncline
Tejonera synform
(c)
COVER (CENOZOIC)
(Fluvial, Aluvial)
VARISCAN SYN-OROGENIC STRATA (CARBONIFEROUS)
Conglomerates, sandstones, lutites and coal (Peñarroya beds) (C_3) (Bashkirian – Moscovian)
Sandstones, lutites, conglomerates, limestones, coal, and rhyolites (Granja de Torrehermosa) (C_2) (Upper Viséan – Serpukhovian)
Slates, meta-greywackes, meta-conglomerates and metabasites (Culm facies) (C_1) (Tournaisian – Upper Viséan to Serpukhovian)
ALLOCHTHONOUS SUTURE ZONE
(Intermediate fault-bounded domains of the Espiel thrust)
Serpentinites (Ophiolitic / Middle Allochthon)
Meta-igneous rocks
AUTOCHTHON (EARLY CAMBRIAN)
(Azuaga Formation)
Quartzites, phyllites
Metasandstones, phyllites
Quartzites
Micro-banded phyllites

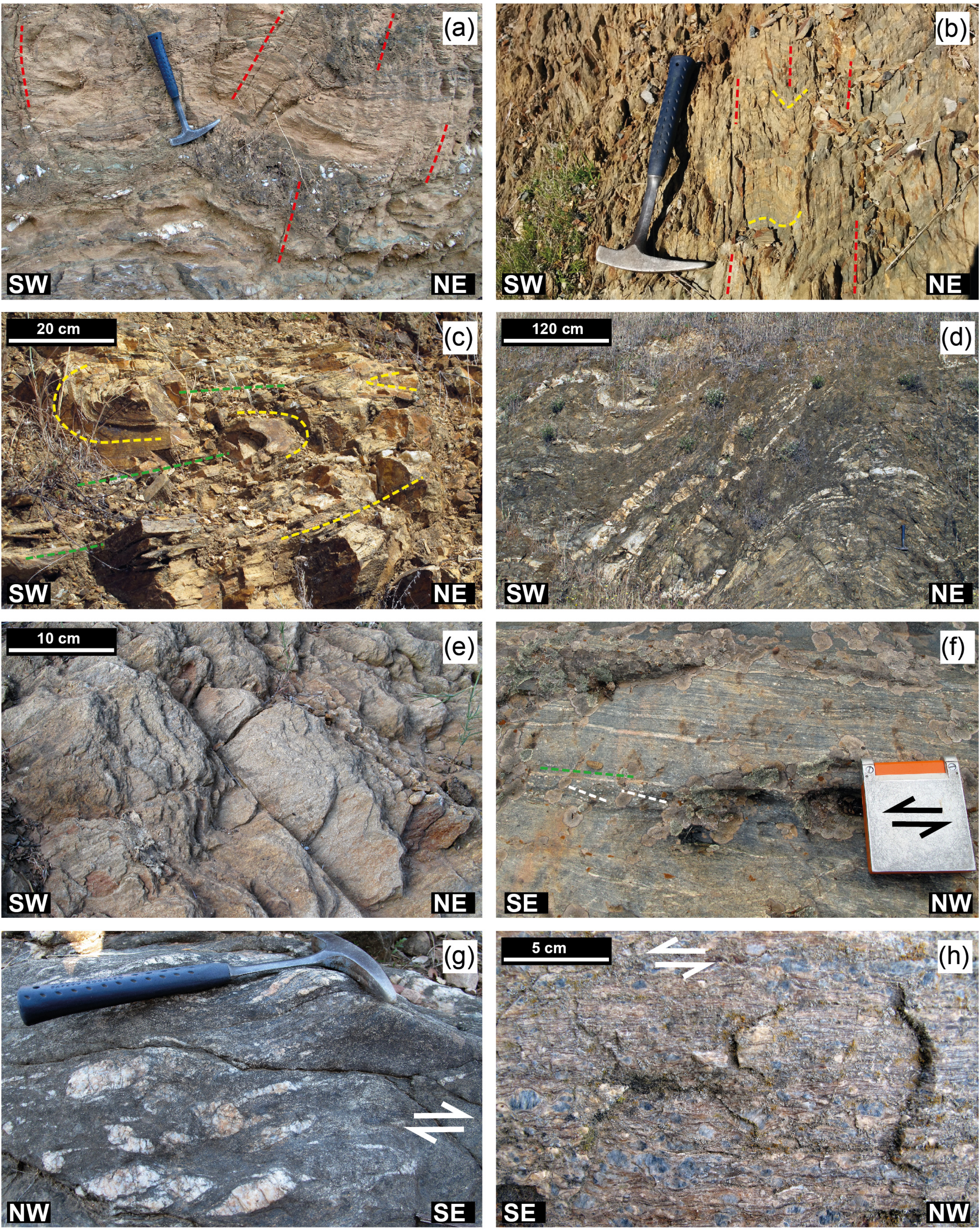

(a)
SW
NE
(b)
SW
NE
20 cm
(c)
SW
NE
120 cm
(d)
SW
NE
10 cm
(e)
SW
NE
(f)
SE
NW
(g)
NW
SE
5 cm
(h)
SE
NW

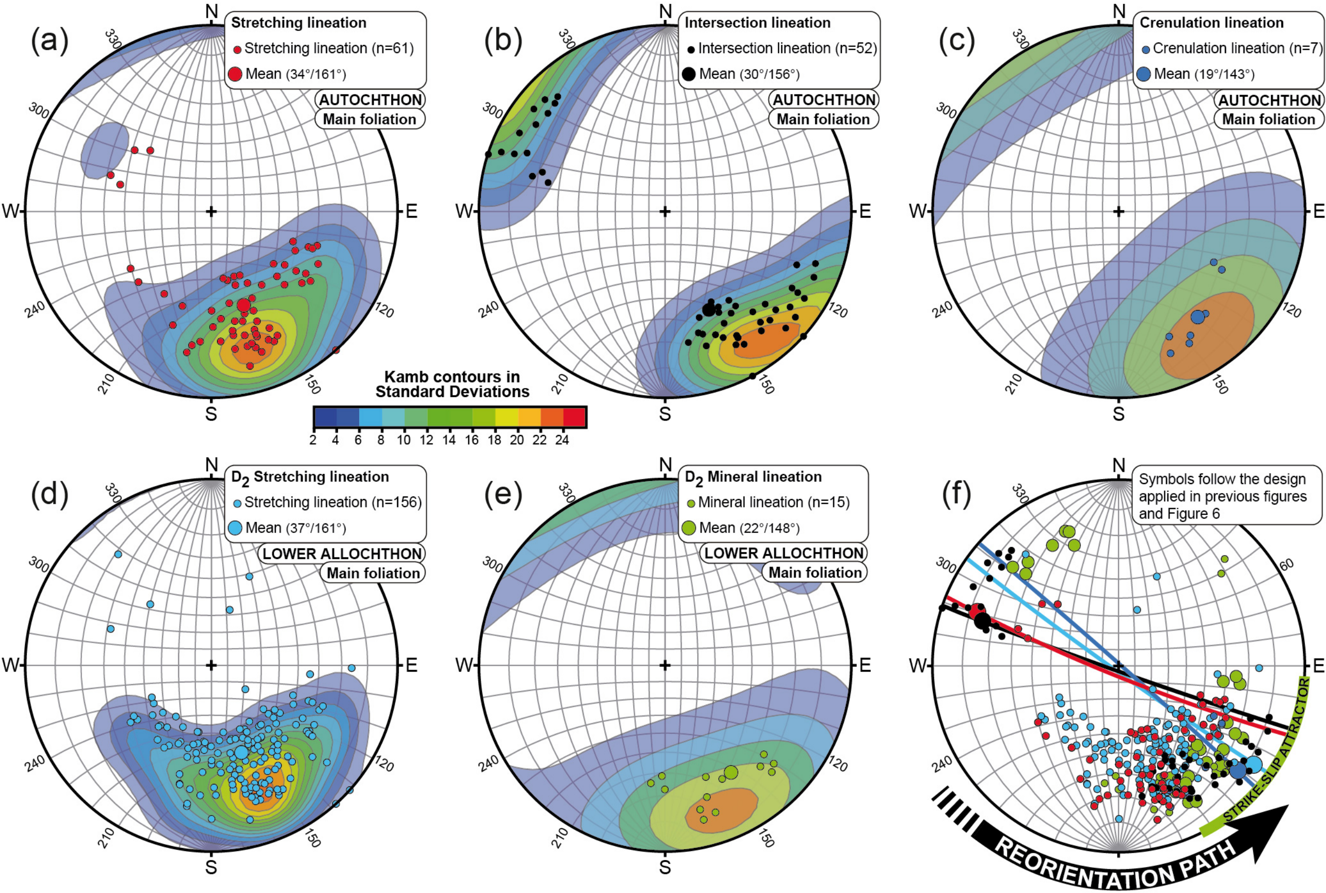

(a)
Stretching lineation
Stretching lineation (n=61)
Mean (34°/161°)
AUTOCHTHON
Main foliation
(b)
Intersection lineation
Intersection lineation (n=52)
Mean (30°/156°)
AUTOCHTHON
Main foliation
(c)
Crenulation lineation
Crenulation lineation (n=7)
Mean (19°/143°)
AUTOCHTHON
Main foliation
Kamb contours in
Standard Deviations
2 4 6 8 10 12 14 16 18 20 22 24
(d)
D2 Stretching lineation
Stretching lineation (n=156)
Mean (37°/161°)
LOWER ALLOCHTHON
Main foliation
(e)
D2 Mineral lineation
Mineral lineation (n=15)
Mean (22°/148°)
LOWER ALLOCHTHON
Main foliation
(f)
Symbols follow the design
applied in previous figures
and Figure 6
STRIKE-SLIP ATTRACTOR
REORIENTATION PATH
N
S
E
W
330
300
240
210
150
120
60

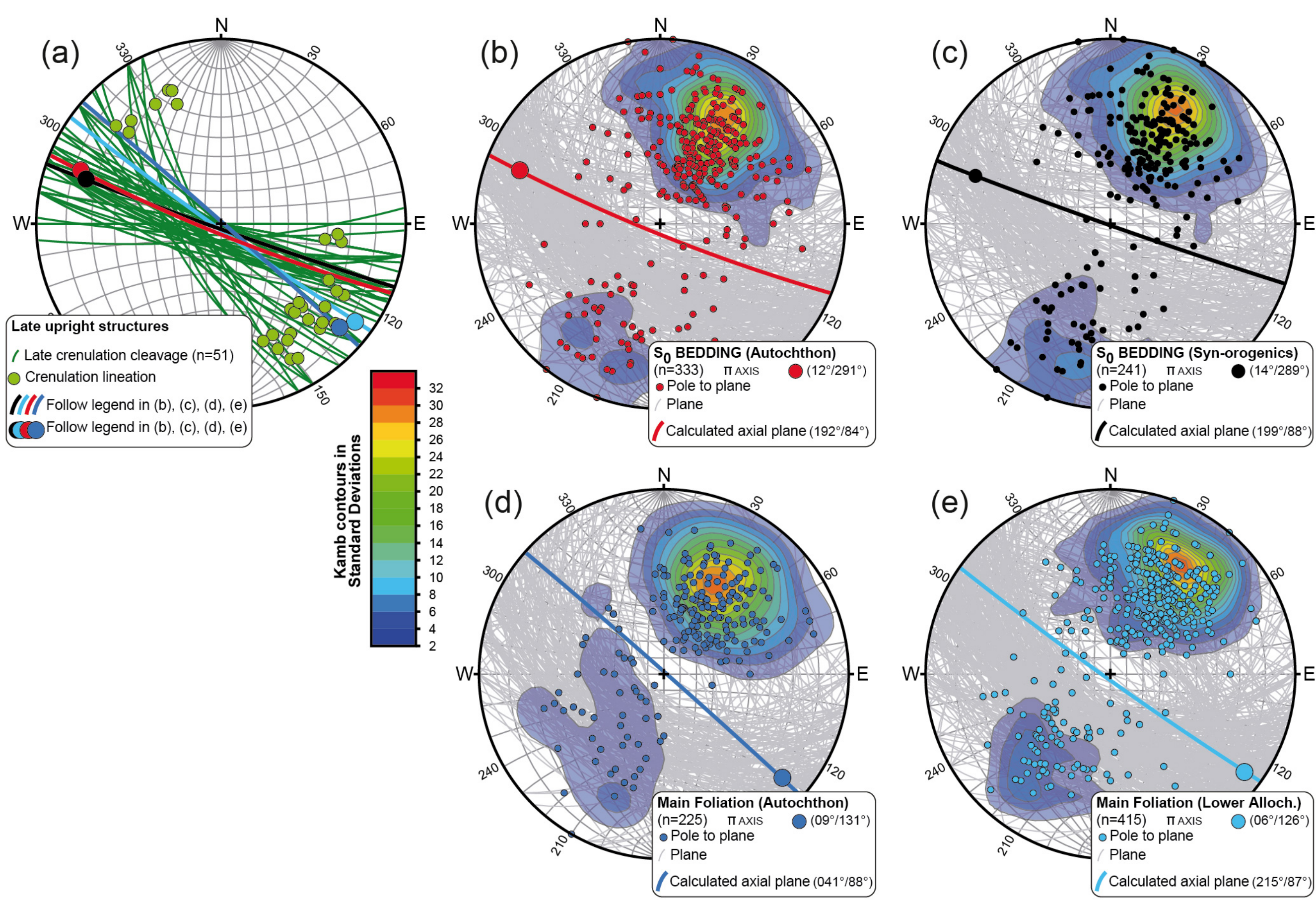
(a)
Late upright structures
Late crenulation cleavage (n=51)
Crenulation lineation
Follow legend in (b), (c), (d), (e)
Follow legend in (b), (c), (d), (e)
(b)
S0 BEDDING (Autochthon)
(n=333) π AXIS (12°/291°)
Pole to plane
Plane
Calculated axial plane (192°/84°)
(c)
S0 BEDDING (Syn-orogenics)
(n=241) π AXIS (14°/289°)
Pole to plane
Plane
Calculated axial plane (199°/88°)
Kamb contours in Standard Deviations
(d)
Main Foliation (Autochthon)
(n=225) π AXIS (09°/131°)
Pole to plane
Plane
Calculated axial plane (041°/88°)
(e)
Main Foliation (Lower Alloch.)
(n=415) π AXIS (06°/126°)
Pole to plane
Plane
Calculated axial plane (215°/87°)

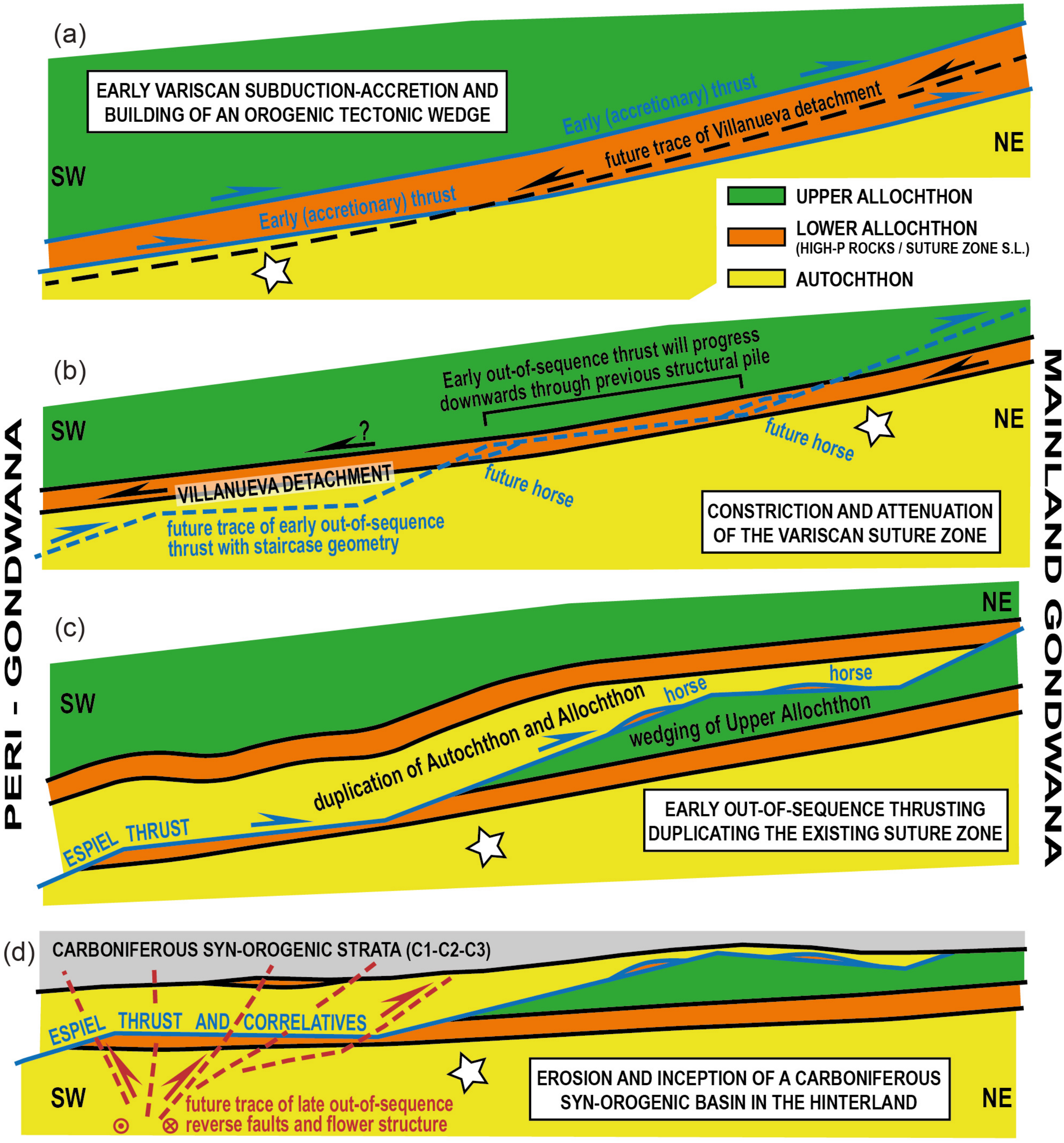

(a)
EARLY VARISCAN SUBDUCTION-ACCRETION AND BUILDING OF AN OROGENIC TECTONIC WEDGE
SW
NE
Early (accretionary) thrust
future trace of Villanueva detachment
Early (accretionary) thrust
UPPER ALLOCHTHON
LOWER ALLOCHTHON
(HIGH-P ROCKS / SUTURE ZONE S.L.)
AUTOCHTHON
(b)
SW
NE
Early out-of-sequence thrust will progress downwards through previous structural pile
?
VILLANUEVA DETACHMENT
future horse
future horse
future trace of early out-of-sequence thrust with staircase geometry
CONSTRICTION AND ATTENUATION OF THE VARISCAN SUTURE ZONE
PERI - GONDWANA
MAINLAND GONDWANA
(c)
SW
NE
duplication of Autochthon and Allochthon
horse
horse
wedging of Upper Allochthon
ESPIEL THRUST
EARLY OUT-OF-SEQUENCE THRUSTING DUPLICATING THE EXISTING SUTURE ZONE
(d)
CARBONIFEROUS SYN-OROGENIC STRATA (C1-C2-C3)
ESPIEL THRUST AND CORRELATIVES
SW
NE
future trace of late out-of-sequence reverse faults and flower structure
EROSION AND INCEPTION OF A CARBONIFEROUS SYN-OROGENIC BASIN IN THE HINTERLAND

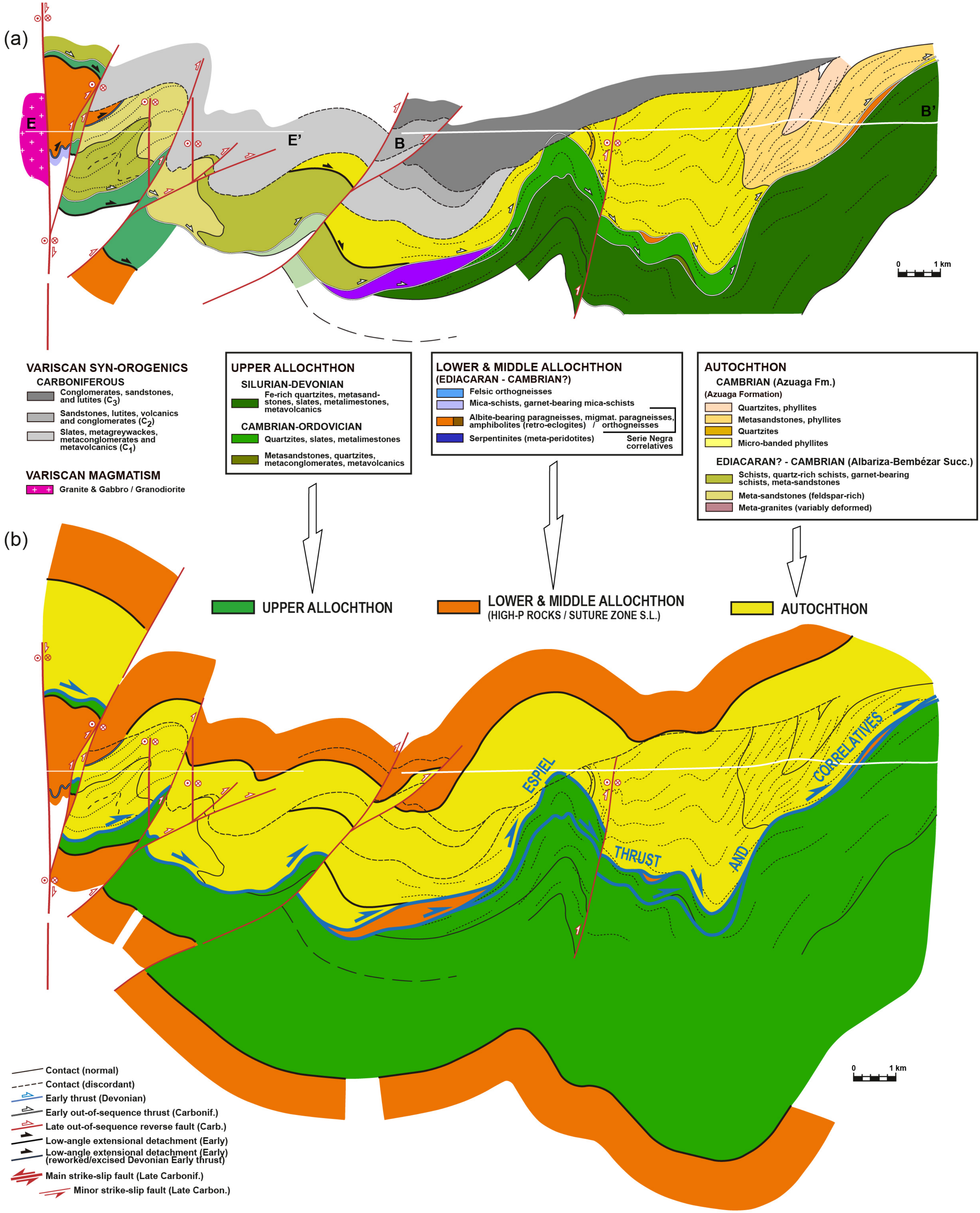
(a)
E
E'
B
B'
0 1 km
VARISCAN SYN-OROGENICS
CARBONIFEROUS
Conglomerates, sandstones, and lutites (C3)
Sandstones, lutites, volcanics and conglomerates (C2)
Slates, metagreywackes, metaconglomerates and metavolcanics (C1)
VARISCAN MAGMATISM
Granite & Gabbro / Granodiorite
UPPER ALLOCHTHON
SILURIAN-DEVONIAN
Fe-rich quartzites, metasandstones, slates, metalimestones, metavolcanics
CAMBRIAN-ORDOVICIAN
Quartzites, slates, metalimestones
Metasandstones, quartzites, metaconglomerates, metavolcanics
LOWER & MIDDLE ALLOCHTHON (EDIACARAN - CAMBRIAN?)
Felsic orthogneisses
Mica-schists, garnet-bearing mica-schists
Albite-bearing paragneisses, migmat. paragneisses, amphibolites (retro-eclogites) / orthogneisses
Serpentinites (meta-peridotites)
Serie Negra correlatives
AUTOCHTHON
CAMBRIAN (Azuaga Fm.)
(Azuaga Formation)
Quartzites, phyllites
Metasandstones, phyllites
Quartzites
Micro-banded phyllites
EDIACARAN? - CAMBRIAN (Albariza-Bembézar Succ.)
Schists, quartz-rich schists, garnet-bearing schists, meta-sandstones
Meta-sandstones (feldspar-rich)
Meta-granites (variably deformed)
(b)
UPPER ALLOCHTHON
LOWER & MIDDLE ALLOCHTHON
(HIGH-P ROCKS / SUTURE ZONE S.L.)
AUTOCHTHON
ESPIEL
THRUST
AND
CORRELATIVES
0 1 km
Contact (normal)
Contact (discordant)
Early thrust (Devonian)
Early out-of-sequence thrust (Carbonif.)
Late out-of-sequence reverse fault (Carb.)
Low-angle extensional detachment (Early)
Low-angle extensional detachment (Early) (reworked/excised Devonian Early thrust)
Main strike-slip fault (Late Carbonif.)
Minor strike-slip fault (Late Carbon.)